NASA TECHNICAL NOTE

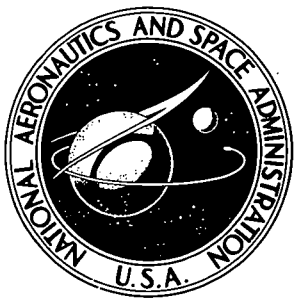

NASA TN D-7311

NASA TN D-7311

A STUDY OF THE THERMOREGULATORY CHARACTERISTICS OF A LIQUID-COOLED GARMENT WITH AUTOMATIC TEMPERATURE CONTROL BASED ON SWEAT RATE: EXPERIMENTAL INVESTIGATION AND BIOTHERMAL MAN-MODEL DEVELOPMENT

by Alan B. Chambers, James R. Blackaby, and John B. Miles

Ames Research Center
Moffett Field, Calif. 94035

NATIONAL AERONAUTICS AND SPACE ADMINISTRATION • WASHINGTON, D. C. • JUNE 1973

1. Report No.	2. Government Accession No.	3. Recipient's Catalog No.
NASA TN D-7311		

4. Title and Subtitle	5. Report Date
A STUDY OF THE THERMOREGULATORY CHARACTERISTICS OF A LIQUID-COOLED GARMENT WITH AUTOMATIC TEMPERATURE CONTROL BASED ON SWEAT RATE: EXPERIMENTAL INVESTIGATION AND BIOTHERMAL MAN-MODEL DEVELOPMENT	June 1973
	6. Performing Organization Code

7. Author(s)	8. Performing Organization Report No.
Alan B. Chambers, James R. Blackaby, and John B. Miles	A-4686
	10. Work Unit No. 970–22–30–13

9. Performing Organization Name and Address	11. Contract or Grant No.
NASA Ames Research Center Moffett Field, California 94035	
	13. Type of Report and Period Covered
12. Sponsoring Agency Name and Address	Technical Note
National Aeronautics and Space Administration Washington, D. C. 20546	14. Sponsoring Agency Code

15. Supplementary Notes

16. Abstract

Experimental results for three subjects walking on a treadmill at exercise rates of up to 590 watts showed that thermal comfort could be maintained in a liquid-cooled garment by using an automatic temperature controller based on sweat rate. The addition of head- and neck-cooling to an Apollo-type liquid-cooled garment increased its effectiveness and resulted in greater subjective comfort. The biothermal model of man developed in the second portion of the study utilized heat rates and exchange coefficients based on the experimental data, and included the cooling provisions of a liquid-cooled garment with automatic temperature control based on sweat rate. Simulation results were good approximations of the experimental results.

17. Key Words (Suggested by Author(s))	18. Distribution Statement
Liquid-cooled garment temperature control Biothermal model of man Liquid-cooled garment effectiveness	Unclassified – Unlimited

19. Security Classif. (of this report)	20. Security Classif. (of this page)	21. No. of Pages	22. Price*
Unclassified	Unclassified	72	$3.00

*For sale by the National Technical Information Service, Springfield, Virginia 22151

TABLE OF CONTENTS

SYMBOLS

The symbols used in the report are grouped according to their use or units of measurement and listed in three separate categories:

Exp: These symbols are used in the discussion included in the section entitled Experimental Investigations

Model: These symbols are used in the discussion included in the section entitled Computer Simulation of Man, the LCG, and the Controller

CSMP: These symbols comprise the basic notation necessary for interpretation of the computer program (CSMP), appendix A

Exp	Model	CSMP	Heat rates, W
H_{ALAT}	H_{ALAT}	HALAT	total latent heat to air
	H_{ATL}		air to LCG
H_{ASENS}	H_{ASENS}	HASENS	total sensible heat to air
		HCTS	core to skin
		HCTM	core to muscle
	H_E		evaporative heat from skin (Winton)
	H_{ER}	HER	evaporative heat through respiration
	H_{ES}	HES	evaporative heat from skin
H_L	H_L	HL	loss through the air ventilation garment
H_{LCG}	H_{LCG}	HLCG	total to LCG
		HMTS	muscle to skin
	H_{SENSR}	HSENSR	sensible heat through respiration
	H_{STA}	HSTA	skin to air
	H_{STL}	HSTL	skin to LCG
H_{TOTAL}	H_{TOTAL}	HTOTAL	total leaving outer garment
			Metabolic rates, W
	M_{BAS}	MBAS	basal
	M_C	MC	total in core

Exp	Model	CSMP	
	M_{EX}	MEX	exercise
	M_M	MM	total in muscle
	M_{SH}		shivering
	M_{TOTAL}	MTOTAL	total in core and muscle
			Thermal exchange coefficients, W/°C
	EX_{ATL}	EXATL	ventilating air to LCG
EX_{AVG}	EX_{AVG}		through the air ventilation garment
	EX_{STA}	EXSTA	skin to air
	EX_{STL}	EXSTL	skin to LCG (total)
	EX_{STLA}	EXSTLA	skin to LCG (accumulated sweat)
	EX_{STLR}	EXSTLR	skin to LCG (at rest)
	EX_{STLX}	EXSTLX	skin to LCG (exercise)
			Conductances, W/°C
	G_A		skin to environment (Winton)
	G_V		core to skin (Winton)
	G_{V1}	GV1	core to muscle (total)
	G_{V1ERR}	GV1ERR	core to muscle (ERR)
	G_{V1P}	GV1P	core to muscle (exercise with rise time)
	G_{V1S}	GV1S	core to muscle (exercise)
	G_{V2}	GV2	core to skin (ERR and total)
	G_{V3}	GV3	muscle to skin (total)
	G_{V3P}	GV3P	muscle to skin (exercise with rise time)
	G_{V3S}	GV3S	muscle to skin (exercise)
			Temperatures, °C
	DT_{REF}	DTREF	change in reference temperature
	T_A		environment (Winton)

Exp	Model	CSMP	
	T_{AAVE}	TAAVE	average air temperature in outer garment
T_{AI}	T_{AI}	TAI	air entering outer garment
T_{AO}	T_{AO}	TAO	air leaving outer garment
T_{BASAL}			set temperature at basal condition
	T_C	TC	core (rectal)
T_{COOL}			cold water supply to proportional valve
T_{DPI}	T_{DPI}	TDPI	dewpoint of entering air
T_{DPO}			dewpoint of exiting air
T_G	T_G	TG	ambient environment (globe)
	T_{LAVE}	TLAVE	average water temperature in LCG
T_{LI}	T_{LI}	TLI	water at LCG inlet
T_{LO}	T_{LO}	TLO	water at LCG outlet
	T_M	TM	muscle
	T_{REF}	TREF	reference
T_S	T_S	TS	skin
T_{SET}	T_{SET}	TSET	prescribed LCG temperature
	T_{VAL}	TVAL	water at proportional valve outlet
T_{WARM}			warm water supply to proportional valve
ΔT_B			variation in mean body temperature with respect to the value at the start of exercise
ΔT_C			variation in rectal temperature with respect to the value at the start of exercise

Feedback Signals and Gains

ERR	ERR	total feedback signal, °C
Core F.B.	FBC	feedback from core, °C
Skin F.B.	FBS	feedback from skin, °C
	GNC	gain for core feedback
	GNS	gain for skin feedback

Exp	Model	CSMP	Heat capacitances, W-sec/°C
	C_C	CC	core
	C_M	CM	muscle
	C_S	CS	skin
			Volume flow rates, liters/min
A_{FR}	A_{FR}	AFR	air through outer garment
	V_R	VR	pulmonary ventilation rate
W_{FR}	W_{FR}	WFR	water through LCG
			Water and water vapor flow rates, g/hr
DWL_{ID}	DWL_{ID}	DWLID	$WV_{OG} - WV_{OGB}$
	S_{R1}	SR1	sweat rate
	S_{R2}	SR2	sweat rate indicator
		SACR	accumulation rate on skin
	W_{ER}	WER	evaporated by respiration
	W_{ES}	WES	evaporated from skin
	W_{ESMAX}	WESMAX	maximum evaporation rate from skin
		WLID	loss indicated at hygrometer
	WV_{IG}	WVIG	entering outer garment
WV_{OG}	WV_{OG}	WVOG	leaving outer garment
WV_{OGB}	WV_{OGB}		leaving outer garment (basal)
			Cumulative amounts of water, g
	S_{ACUM}	SACUM	total accumulated sweat at any time
	S_{ACMAX}	SACMAX	maximum value attained by S_{ACUM}
		STOTAL	total sweat to skin
		WERTOT	total respiratory water loss
		WLTOT	total water loss

Exp	Model	CSMP	
			Water vapor pressures, mm Hg
	P_{WAVE}	PWAVE	average for air in outer garment
	P_{WC}	PWC	saturated air at core temperature
	P_{WH}	PWH	as measured at hygrometer
P_{WI}		PWI	air entering outer garment
P_{WO}		PWO	air leaving outer garment
		PWS	saturated air at skin temperature
			Miscellaneous
	A_{WET}	AWET	fractional wetted area of LCG
E/P			signal to proportional valve operator, volts
	V_{TM}	VTM	treadmill speed, m/sec

A STUDY OF THE THERMOREGULATORY CHARACTERISTICS OF A LIQUID-COOLED GARMENT WITH AUTOMATIC TEMPERATURE CONTROL BASED ON SWEAT RATE: EXPERIMENTAL INVESTIGATION AND BIOTHERMAL MAN-MODEL DEVELOPMENT

Alan B. Chambers, James R. Blackaby, and John B. Miles[1]

Ames Research Center

SUMMARY

The thermal comfort of an astronaut in a pressure suit during extravehicular activity is maintained primarily by use of a liquid-cooled garment in conjunction with a forced air or forced oxygen ventilating system. Temperature regulation has been achieved in past Apollo flight operations by manual control, but several methods of automatic control have been studied. For the present investigation, an automatic temperature controller based on the sweat rate — or more precisely, the total evaporative water loss rate — of exercising subjects was developed.

Tests of the controller were conducted with three male subjects walking on a level treadmill at steady or varying exercise rates ranging from 220 to 590 W. Physiological measurements were made and subjective comfort data were recorded for all the tests. Liquid-cooled garment temperature regulation was dependent only on changes of humidity at the outlet of the air-ventilated simulated pressure suit worn by the subjects. The response, stability, and effectiveness of the automatic temperature controller were adequate to maintain the subjects in a comfortable thermal state throughout the tests.

The test data were utilized to refine an existing biothermal model of man designed to provide digital computer simulation of the thermal processes of exercising subjects. The model was extended to include the effects of the liquid-cooled garment, air ventilation garment, and automatic control of the liquid-coolant temperature based on the subject's evaporative water loss rate. The metabolic and thermal characteristics of the model developed matched the data of the experimental investigation in all important respects.

INTRODUCTION

During extravehicular activity (EVA), astronauts are equipped with liquid-cooled garments (LCG) for the purpose of removing body heat to maintain thermal comfort. These garments are net-like in construction, fit closely to the skin, and contain many small tubes through which chilled water flows. Nunneley (ref. 1) has described the functioning of these suits and the original need for them when cooling by gas ventilation alone was inadequate.

---

[1] Professor of Mechanical and Aerospace Engineering, University of Missouri-Columbia (National Research Council Associate, Ames Research Center, 1971)

An important consideration when using an LCG is the control of the supply-water temperature. In the Apollo missions, the temperature of the water has been regulated using a three-way manual valve which controls the amount of water that is bypassed for cooling to the heat sink (a sublimator located on top of the portable life support system). Removing this control function from the astronaut is desirable not only from the standpoint of relieving an already busy astronaut, but also because an astronaut preoccupied with a challenging task may not be a good judge of his own thermal state.

Various investigators have attempted to develop an automatic temperature controller for the LCG. The principal devices may be briefly described in terms of their essential functioning as follows: 1) the metabolic rate controller, which depresses the LCG inlet temperature with increasing oxygen consumption (refs. 2 and 3); 2) the fluidic controller, which attempts to maintain a constant skin temperature (refs. 4 and 5); 3) the differential temperature controller, which seeks to maintain the skin at a prescribed temperature level for a given heat-removal rate by the LCG (determined by the differential temperature across the LCG) (refs. 6 and 7); and 4) the ear canal temperature controller, which attempts to hold a constant mean body temperature (ref. 8). Chambers (ref. 9) has discussed in some detail the features and limitations of the first three of these prior LCG controller development efforts. The fourth, the ear canal temperature controller, suffers some of the same shortcomings as the others, including the requirement that sensors need to be attached to the astronaut.

The objective of the present program was to avoid the deficiencies of previous concepts and develop an LCG temperature controller that remotely senses the astronaut's desire for cooling as a function of his sweat rate, or, more precisely, his total evaporative-water-loss rate during exercise. This report discusses the logic of the new LCG controller, its operation under experimental test conditions, and a mathematical model of its interaction with the astronaut.

The authors wish to acknowledge the assistance of Ronald Schmickley, Brian Glusovich, and Jane Jordan of Programming Methods, Inc., in the development and implementation of the on-line computer program used in the experimental investigation and the computer plotting program utilized to display the performance characteristics of the theoretical biothermal model of man.

CONTROLLER AND SYSTEM MODELS

The concept of automatic control of the LCG inlet temperature based on sweat rate is compatible with the interdependence of physiological and subjective comfort phenomena illustrated in figure 1. The figure includes the results of an unpublished study conducted in the Environmental Control Research Branch at NASA Ames Research Center and relates to subjects wearing an Apollo-type LCG. It can be seen that for optimum comfort, the skin temperature should be lowered in conjunction with increasing workload and an increase in sweat rate.

The manner in which man's physiological temperature control processes are linked to the action of the LCG and the automatic LCG temperature controller of the present investigation is illustrated schematically in figure 2. A metabolic disturbance, for example, change in work rate, affects man's thermoregulatory system so that there is a tendency for sweat rate and skin temperature T_S to change accordingly. The man is considered to be wearing an LCG and an air-ventilated

garment (such as an astronaut's pressure suit); thus for control purposes, a change in sweat rate can be measured as a change in the moisture content of the ventilation air between the inlet and outlet conditions. Sweat rate is the prime input to the controller, and any change in sweat rate – or evaporative water loss, as noted in figure 2 – results in a counteracting change in the temperature T_{LI} of the inlet liquid to the LCG. Thus, the cooling effectiveness H_{LCG} of the LCG, which is a function of the temperature difference ΔT between T_{LI} and T_S, is altered as a function of sweat rate.

Further details of the development and experimental operation of the controller will be presented in a later section of this report. The preceding discussion has been intended only to outline the primary elements of interaction of the physical and physiological parameters relating to the model of man, the LCG, and the LCG temperature controller. This outline describes only the basic causes and effects concerned with maintaining a space-suited man in a comfortable thermal state; it is not sufficient either for a detailed analysis of the thermoregulatory processes involved, or for an analytical design of the elements of the cooling system.

In order to satisfy such detailed requirements, a complete model has been developed as portrayed in figure 3. This model includes all the elements of consequence for the study of the heat balance of man, the LCG, the air ventilation suit, the environment, and the LCG temperature controller. The derivations and/or selections of heat production rates, heat transfer rates, mass flow rates, thermal conductivities, etc. necessary for the practical utilization of the model are included later in this report in the section on Computer Simulation of Man, the LCG, and the Controller.

EXPERIMENTAL INVESTIGATIONS

A test program was conducted to determine the extent to which the automatic temperature controller was capable of maintaining an exercising subject in a comfortable thermal state. The program consisted of two series of treadmill exercise experiments with three subjects. The subjects wore a snug-fitting liquid-cooled garment (LCG) and a loose-fitting air ventilation garment (AVG) simulating an astronaut's pressure suit. An Apollo-type LCG was used for the first of the two series of exercise experiments, while for the second an LCG was used that was fabricated in the same manner as the Apollo-type, but included a provision for head- and neck-cooling. Details concerning the garments, instrumentation, temperature controller, test program, and experimental results are included in the following sections.

Liquid-Cooled Garments

The first series of tests utilized a standard Apollo-type LCG (fig. 4 (a)) with approximately 90 m of tubing in contact with the subject's skin surface; this LCG weighed about 1.7 kg when filled with water. The second LCG used was similar to the Apollo-type garment, but included head- and neck-cooling (fig. 4 (b)). This modification of the standard LCG increased the tubing length by about 6 m and resulted in an LCG weighing about 2.1 kg when filled with water.

Air Ventilation Garment

The air ventilation garment (AVG) was fabricated of rubberized material with rubber boots and gloves and a sealed helmet (fig. 5 (a)). In addition to the fittings required for inlet and outlet air flow, the AVG included bulkhead fittings for the electrical instrumentation, the communication system, and the inlet and outlet water flow lines required by the LCG.

Inlet air was conducted to the hands and feet as well as over the top of the head down onto the face (fig. 5 (b)). Table I shows the ventilation duct dimensions and the relative distrubution of air flow in the AVG. All ventilation air exited the AVG in the rear at the outlet air connector. The average air pressure inside the AVG during operation was 5.3 cm H_2O, gauge.

TABLE I.– FLOW DISTRIBUTION CHARACTERISTICS AND AIR SUPPLY TUBE DIMENSIONS FOR AIR VENTILATION GARMENT

	Head	Right arm	Left arm	Right leg	Left leg
Flow, percent	54	10	13	11	12
Diameter, cm	2.5	1.27	1.27	1.27	1.27
Length, m	1.2	1.4	0.76	1.0	0.92

Apparatus and Instrumentation

The apparatus and instrumentation utilized in the experiments are illustrated in figure 6. Electrical instrumentation for the subjects consisted of an electrocardiograph (ECG), six skin temperature thermistors, and a rectal temperature thermistor. The locations of the six skin temperature thermistors were: (1) calf of the left leg; (2) anterior left thigh; (3) chest; (4) back; (5) upper right arm, outside; and (6) right forearm, inside.

In addition to the suited and instrumented subject, figure 6 also shows the AVG air supply system, the dew point measurement system, the LCG water supply system, the LCG temperature controller, and the treadmill. The figure also depicts the instrumentation associated with these systems and shows which data were routed to the remote data collection, recording, and computing equipment.

In the AVG air supply system, ambient air was pumped through a liquid-to-air heat exchanger where it was cooled to approximately 0°C; condensed moisture was separated from the air stream. A portion of the air flow was then diverted (by use of a manually operated 3-way diversion valve) through a constant-power electric heater, the cold and warm air flows were recombined, the total flow was measured, and the total flow conducted through an insulated flexible hose to the AVG. The system provided an essentially constant air flow rate of 29 m^3/hr with a temperature of 18° C ± 1° C at the AVG inlet. The flow rate was manually inserted in the data collection system as a constant. The dew point temperature of the air supplied to the AVG, T_{DPI}, was measured before each test run using the dew point hygrometer, and this value was also manually inserted in the data collection system as a constant. The temperatures in the inlet to the AVG and the outlet from the

AVG, T_{AI} and T_{AO}, respectively, were measured by thermistors and recorded continuously during the tests, and a sample of the outlet air was pumped to the dew point hygrometer to provide a continuous measure of the outlet air dew point temperature, T_{DPO}. The hygrometer could accept only a low flow rate, that is, 1 liter/min or less. In order to reduce the lag time of this portion of the control system, a fairly high sample flow rate was pumped from the AVG outlet (of the order of several liters/min) but less than 1 liter/min was directed to the hygrometer. An electrical signal output from the dew point hygrometer was delivered to the LCG controller (analog computer) where it was amplified and scaled as required for use in the controller and as an input to the data collection system.

The water flow to the LCG was supplied through a temperature regulating system as shown in figure 6. A constant flow rate was maintained through the heater and chiller by means of throttling valves, so that a stable supply of warm and cool water was available at the 3-way mixing valve at all times. The pressure relief valves were set so that with either full warm or full cold water flow through the mixing valve, the flow rate to the LCG was 1.89 liters/min. The excess heated or cooled water was bypassed to the drain. When regulated in this manner, the flow rate to the LCG was essentially constant throughout the mixing range of the valve. The flow rate was inserted in the data collection system as a constant, and the inlet and outlet water temperatures at the LCG, T_{LI} and T_{LO}, respectively, were measured by thermistors and recorded automatically. Details of the automatic temperature controller and mixing valve operation will be discussed in a later section of the report.

The treadmill incorporated a velocity meter with remote electrical output capability; thus, the treadmill speed was continuously inserted in the data collection system. Another input to the data collection system was the test chamber temperature, T_G, as measured by a thermistor suspended in the center of a black, 15-cm diameter, thin-walled copper sphere.

Data Handling System

The data collection, recording, and computing system incorporated analog signal receiving and conditioning instruments; analog-to-digital conversion equipment; a sequential data sampling device; raw data print-out, paper tape punch, and magnetic tape production equipment; on-line and/or off-line electronic computing capability; and off-line electronic plotting capability. The data indicated in figure 6 were recorded at 1-minute intervals; the raw data collected were typed at the test director's station as they were being sampled, as well as being recorded on paper and magnetic tape. All performance parameters of interest were computed on-line and were recorded on magnetic tape; selected parameters were typed out at the test director's station to permit constant surveillance of the condition of the subject and the progress of the test. At the conclusion of the test program the computed data stored on magnetic tapes were further analyzed and combined using electronic computing equipment and computer-generated plots of the data were printed. Selected examples of the computer-plotted data are included in the Experimental Results and Discussion of this section.

LCG Controller and Mixing Valve Operation

The relation of the LCG temperature controller (analog computer) to the 3-way mixing valve and the rest of the experimental equipment is illustrated schematically in figure 6. Details of the controller are shown in figure 7.

Inputs to the controller included thermistor signals from the warm and cool water supplies to the mixing valve and from the dew point hygrometer, as well as manual inputs of water vapor flow rate during basal condition WV_{OGB}, basal LCG inlet temperature T_{BASAL}, and a dc voltage range associated with the slope of the mixing valve characteristic as discussed later in this section. Outputs from the controller included the dew point temperature at the outlet from the AVG, T_{DPO}, and the required set temperature computed for the LCG inlet water, T_{SET}, both of which were inserted in the data collection system. In addition, a voltage signal E/P was generated which, operating through the electric-to-pneumatic transducer, positioned the 3-way mixing valve to provide water at the LCG inlet at a temperature T_{LI} equal to T_{SET}. The electric-to-pneumatic transducer accepted electrical signals between 0 and 10 V dc and provided a corresponding pneumatic pressure to cause full stroking of the mixing valve.

As depicted in figure 8, the mixing valve operating characteristic was essentially a straight line, except for a small extent at each end of the stroke. A mechanical bias was available in the valve operator and was adjusted to eliminate the flat portion of the characteristic at the cool, or zero-voltage, end. An upper voltage was then determined empirically which would limit valve operation to the essentially straight-line portion of the characteristic while still providing water to the LCG at practically the warm supply temperature. Thus, a signal range less than 10 V (approximately 8 V dc) was determined which would provide the full temperature capability of the mixing valve, but would limit its operation to the straight portion of its characteristic. This signal range was inserted manually as a constant in the temperature controller.

The signals from the warm and cool water supply thermistors and from the dew point hygrometer were amplified in the controller and scaled as required to provide usable dc voltages analagous to T_{WARM}, T_{COOL}, and T_{DPO} as indicated on the diagram in figure 7. The E/P signal range was divided by the difference between the warm and cool water temperatures to obtain the slope of the mixing valve characteristic:

$$\text{SLOPE} = \frac{\text{E/P Signal Range}}{(T_{WARM} - T_{COOL})} \tag{1}$$

The set temperature required for the water supply to the LCG, T_{SET}, was computed in the LCG controller based on the sweat rate of the subject. Figure 7 shows schematically how sweat rate was based on T_{DPO}. Sweat rate, in this context, included all of a subject's evaporative water loss – both sensible (sweating) and insensible (nonsweating).

At the start of a test, a subject's evaporative water loss rate at rest was balanced by the manual input WV_{OGB} such that the initial output of operational amplifier A1 was zero. For this same resting condition, an empirically determined, comfortable LCG inlet temperature, T_{BASAL} was inserted manually at operational amplifier A2. Thus, at the start of each test run the output of A2, which was analogous to the set temperature T_{SET} for the LCG inlet water, was equal to T_{BASAL}. For the present tests, T_{BASAL} was 32.2° C.

As a subject exercised, this evaporative water loss rate increased from the resting value; this increase resulted in an increase of the output of operational amplifier A1, analogous to an increase

in evaporative water loss rate DWL_{ID}. This increase in water loss rate was modified by the proportionality constant K such that the product $KXDWL_{ID}$ represented the decrease in the LCG inlet temperature necessary to maintain the subject in a thermally comfortable state. The proportionality constant K was determined in preliminary tests [K = 0.1325 (°C)/(g/hr)].

The following equation was programmed in the controller for the computation of water vapor rate leaving the AVG:

$$WV_{OG} = (0.285)(A_{FR})\left(30^{0.018\ T_{DPO}}\right) \tag{2}$$

Included in equation (2) is an approximation to the relationship between dew point temperature and water vapor pressure in air at standard sea level pressure over the range of temperatures of interest in the tests.

The difference between the analog voltages representing T_{SET} and T_{COOL} was obtained from operational amplifier A3 as shown in figure 7. This difference, multiplied by the slope of the mixing valve characteristic (eq. (1)), produced the control voltage signal E/P to operate the mixing valve.

This controller, in conjunction with the 3-way mixing valve, was capable of rapid response to changes in a subject's sweat rate; the LCG inlet temperature T_{LI} closely matched the computed temperature T_{SET}. Accurate performance was not dependent on the accurate maintenance of constant warm and cool water supply temperatures to the mixing valve. During a test run, T_{WARM} typically varied from 35 to 40° C and T_{COOL} varied from 1 to 5° C.

Test Procedure

Typically, two tests a day could be completed, the first starting at about 9:00 a.m., and the second at about 1:00 p.m.; however, no subject was tested more than once a day. When a subject reported to the laboratory he undressed, inserted the rectal thermistor, and was weighed. The skin thermistors and ECG electrodes were then attached and the LCG put on. The outer air ventilating garment, less helmet and gloves, was then donned and the subject entered the test chamber. The dressing procedure took approximately one hour. No food or liquids were given to the subjects between the initial weighing and the completion of the test.

Upon entering the chamber, the subject's AVG, LCG, instrument umbilicals, and communication system were connected. The inlet water to the LCG was regulated at 32.2° C and the inlet air temperature to the ventilation suit, T_{AI}, was 18° C. The subject was seated prior to the start of the test and all systems (LCG, ventilation, instrumentation, data collection, etc.) were checked to verify proper operation before the helmet and gloves were donned. This final checkout usually took about 10 minutes. With all systems operational and the subject seated the formal test was initiated with the start of the chosen activity schedule (i.e., t=0 min). Test data were recorded at 1-minute intervals and the subject was asked, at 5-minute intervals, to indicate his feelings of comfort and thermal sensations.

At the completion of the activity schedule (t=85 min) the helmet and gloves were removed, the umbilicals were disconnected and the subject was taken from the test chamber; he then removed the AVG, LCG, electrodes and skin thermistors and the second weighing was performed. This weighing occurred about 2 hours and 15 minutes after the initial weighing and completed the test.

Subjective Evaluation of Comfort

During each test the subject was requested to evaluate his feelings of comfort and thermal sensation in terms of the scales shown in table 2. With this dual scale it was possible to indicate combined sensations such as cool and comfortable or slightly cool and uncomfortable (ref. 10). The subjects were instructed to make the sensory estimations in terms of whole body sensations, not individual areas such as limbs or head.

TABLE 2.– SCALES OF SUBJECTIVE COMFORT AND THERMAL SENSATIONS

Scale of comfort sensation	Scale of thermal sensation
1. Comfortable	1. Hot
2. Slightly uncomfortable	2. Warm
3. Uncomfortable	3. Slightly warm
	4. Neutral
	5. Slightly cool
	6. Cool
	7. Cold

Subjects

Three male subjects (VAC, WMC, RHD) were used in the experiments. Their physical and physiological characteristics are presented in table 3. Body surface area and percent body fat were

TABLE 3.– PHYSICAL AND PHYSIOLOGICAL CHARACTERISTICS OF THE TEST SUBJECTS

Subject	Age, yr	Height, cm (in.)	Weight, kg (lb)	Surface area m^2, (ref. 11)	Average skinfold thickness, mm		Body fat, percent (ref. 12)	Maximum O_2 uptake, liters/min
					Thigh	Subscapula		
VAC	22	176 ($69\frac{3}{8}$)	72.0 (158)	1.88	7.2	6.0	6.3	4.25
WMC	22	186 ($73\frac{1}{8}$)	80.5 (177)	2.05	12.3	12.0	11.8	Not measured
RHD	28	178 (70)	73.8 (162)	1.92	5.4	8.7	6.7	5.1

estimated in the manner described in references 11 and 12, respectively. Subjects VAC and RHD were experienced participants in physiological tests. Subject WMC was pursuing a personal physical fitness program, but had not previously participated as a physiological test subject.

Activity Schedule and Metabolic Rate

Six activity schedules, as illustrated in figure 9, were used in the two series of tests. For the first series using the Apollo-type LCG, test numbers 1 through 6 were assigned to designate activity schedules I through VI, while in the second series in which the modified LCG was used, these same activity schedules were denoted as test numbers 7 through 12, respectively. All the activity schedules required the subject to exercise on a level treadmill. During activity schedule I, II, and III (fig. 9(a), (b), and (c)) the subject remained seated for the first 20 minutes, walked at the rate specified (1/2, 1, and 1-1/2 m/sec for schedules I, II, and III, respectively) for 45 minutes, then sat for the remainder of the test period.

Activity schedule IV (fig. 9(d)) started with a 20-minute rest period, then had a 30-minute period of strenuous exercise (2 m/sec walk) and a 35-minute terminal rest period. Schedule V (fig. 9(e)) started with a 15-minute rest period, then had three 10-minute exercise periods (1, 1-1/2, and 1 m/sec, respectively) separated by 10-minute rest periods and concluded with a 20-minute terminal rest period. Schedule VI (fig. 9(f)) began with a 15-minute rest period and ended with 20 minutes of rest. For the first 15 minutes of exercise, the rate was increased from 1/2 to 1-1/2 m/sec as indicated; this was followed by 10 minutes of rest, then 15 more minutes of exercise at a decreasing rate – 1-1/2 to 1/2 m/sec – and five more minutes of rest, then 5 minutes of strenuous exercise at 2 m/sec before the terminal rest period.

For all the tests, the LCG inlet temperature was manually set at 32.2° C for most of the initial rest period. During this time, the output of amplifier A1 of the automatic temperature controller (fig. 7) was monitored and the basal water loss rate input WV_{OGB} was adjusted to maintain the output of amplifier A1 at zero. Then during the last 5 minutes of the initial rest period, with a basal temperature T_{BASAL} input of 32.2° C and amplifier A1 at zero, controller operation was switched to the automatic mode where it remained until the end of the schedule; no further manual adjustments were made.

Separate tests were conducted with two of the subjects (VAC and RHD) to measure the metabolic rates developed by the various treadmill exercise rates. For these tests the face plate was removed from the helmet of the AVG to permit respiratory gas collection. The subjects followed the same preparatory procedure as during the regular tests, donned the LCG and the AVG, entered the test chamber, and connected the various umbilicals. Metabolic rates were measured at rest (sitting) and at treadmill speeds of 1/2, 1, 1-1/2, and 2 m/sec. The subjects remained at each exercise level for at least 15 minutes prior to collection of expired gas samples. The gas samples were collected for 2 to 3 minutes and were analyzed by standard techniques yielding minute volume, oxygen uptake, respiratory quotient (RQ), and carbon dioxide production. The results are shown in figure 10. Also included in figure 10 are data from two other sources (refs. 13 and 14) which corroborate the metabolic levels measured for the present tests.

Calculated Variables

From the measured experimental variables previously discussed the following quantities were calculated: average skin temperature, T_S; latent heat transferred from the subject, H_{ALAT}; total sensible heat transferred to the air, H_{ASENS}; total heat transferred to the LCG, H_{LCG}; heat transferred from the air-ventilation suit to the environment, H_L; and the total heat transferred from the subject, H_{TOTAL}. These parameters were calculated using the following algorithms:

$$T_S = 0.2\,T_{LEG} + 0.19\,T_{THIGH} + 0.13\,T_{FOREARM} + 0.06\,T_{ARM} + 0.21\,(T_{CHEST} + T_{BACK}) \tag{3}$$

$$H_{LCG} = 69.6\,W_{FR}\,(T_{LO} - T_{LI}) \tag{4}$$

$$H_{ASENS} = 0.01995\,A_{FR}\,(T_{AO} - T_{AI}) \tag{5}$$

$$H_{ALAT} = 0.0402\,A_{FR}\,(P_{WO} - P_{WI}) \tag{6}$$

$$H_L = EX_{AVG}\left\{\frac{T_{AI} + T_{AO}}{2} - T_G\right\} \tag{7}$$

$$H_{TOTAL} = H_{LCG} + H_{ASENS} + H_{ALAT} + H_L \tag{8}$$

Equation (3) represents a weighted average skin temperature, as proposed in reference 15. Equations (4), (5), and (6) are based on standard energy balances from the inlet to the outlet of the AVG or the LCG. The basis for equation (7), which predicts heat loss through the AVG, is discussed in appendix B.

Experimental Results and Discussion

The results of the 36 experiments (12 tests with each of the three subjects) are shown in figures 11 through 24. The quantitative data, grouped by test number, are presented in figures 11 through 22. The data depicting the subjective evaluations of thermal sensation, grouped according to LCG type (the Apollo-type LCG for tests 1-6, and the modified LCG for tests 7-12), are presented in figures 23 and 24.

The data plotted in figures 11 through 22 include the following parameters (reading from bottom to top of each figure): treadmill speed; latent heat loss rate, H_{ALAT}; LCG inlet temperature, T_{LI}; rate of heat removal by the LCG, H_{LCG}; average skin temperature, T_S; rectal temperature variation ΔT_C; and mean body temperature variation, ΔT_B. Each plot (except for treadmill speed) shows the average value of the variable for the three subjects and the average value plus and minus one standard deviation.

Treadmill speed is the only independent variable in the experiment. It was manually adjusted according to the activity schedules discussed previously. In all tests the subjects remained seated until 20 seconds before the start of any treadmill exercise period and were seated within 20 seconds after the termination of each exercise period.

The latent heat rate curves are based on the total change in water vapor content of the ventilating air from the AVG inlet to outlet. Accordingly, these curves represent the sum of respiratory water loss plus that portion of the subjects' sweat output which was being evaporated by the ventilating air. At the lower work rates essentially all the subjects' sweat was being evaporated; however, at the higher rates, more sweat was secreted than could be immediately evaporated. This effect is attributed to mass transfer limitations between the LCG-covered skin and the ventilating air, since the ventilating air did not reach saturation during any of the tests. The results of the sweat accumulation conditions at the higher work rates are evidenced by the data for tests 4 and 10, which show that the total latent heat transfer to the ventilating air H_{ALAT} reached a maximum and leveled off even though the subjects' core temperatures continued to rise with continued exercise.

A rise in latent heat loss rate H_{ALAT} occurred immediately after the onset of exercise; this may be logically attributed to an increase of insensible water loss from the respiratory tract resulting from increased pulmonary ventilation as exercise was begun. Following this initial rise, the latent heat loss rate tended to level off for a short time until active sweating began.

After termination of exercise, H_{ALAT} decreased abruptly, then continued decreasing gradually to a final level that was still higher than the initial resting level even at the termination of the test. The initial decrease in H_{ALAT} is attributed to the reduction in pulmonary ventilation as exercise was terminated. The continuing gradual decay resulted from the combined effects of diminishing sweat output and continued evaporation of the accumulated sweat. The failure of H_{ALAT} to return to the initial level is attributed to the existence of residual sweat as confirmed by visual inspection of the subjects and the LCG after completion of a test.

The LCG inlet temperature can be seen to vary with the latent heat loss. The variation of LCG cooling provided by the automatic controller corresponds directly to the subject's personal demand for cooling. The LCG inlet temperature is lowered when the subject's normal physiological mechanisms demand cooling, and likewise, the LCG inlet temperature is raised only when those mechanisms call for less cooling.

The calculated data for heat transfer rate to the LCG, H_{LCG} appears irregular in comparison with the other data plotted in figures 11 through 22, although the trend of the H_{LCG} curves corresponds well with the latent heat rate curves, especially in tests 5, 6, 11, and 12. The erratic nature of the H_{LCG} data results from the combined effects of transportation lags of the water from the inlet to the outlet of the LCG and the minute-by-minute summation and computation technique employed.

The skin temperature follows changes in the LCG inlet temperature and therefore, changes in the latent heat loss curves. For measurement of skin temperature, thermistors were attached to the subjects prior to donning the LCG. No attempt was made to orient the thermistor positions relative to the LCG tubing; some care should therefore be exercised in interpreting the skin temperature data. Similar care should be used when analyzing mean body temperatures which are calculated from the skin and rectal temperatures.

The rectal and mean body temperatures were normalized by the values measured at the start of exercise for each test (at t = 20 minutes in tests 1-4 and 7-10, and t = 15 minutes in tests 5, 6, 11, and 12) to yield ΔT_C and ΔT_B. In tests 1-3 and 7-9, the rectal temperature generally appears to have reached a maximum by the end of the exercise period indicating that thermal equilibrium was established. In tests 4 and 10, however, the rectal temperatures were still increasing when exercise was terminated, indicating that thermal equilibrium had not been reached.

Variations in mean body temperature were small and ranged around zero in all tests except 4 and 10, in which the mean body temperature remained depressed even after termination of exercise. In these tests, the delayed evaporation of water from the subject and the LCG fabric resulted in a depressed LCG inlet temperature and therefore, a reduced skin temperature. The low skin temperature then kept the calculated mean body temperature low. Even with this apparent depression of the mean body temperature, none of the subjects expressed any signs of thermal discomfort.

The subjective evaluations of thermal sensation shown in figures 23 and 24 indicate a greater variability during the tests with the Apollo-type LCG than with the modified (hooded) LCG. This is primarily due to the more effective cooling realized by exposing the whole body to a uniform temperature, as contrasted to the method of cooling which exposes the head and neck to a different temperature than the remainder of the body. The improved characteristics of the modified LCG, indicated by the "neutral" responses with respect to thermal sensation, shows the desirability of adding head- and neck-cooling to the Apollo-type LCG.

With respect to the subjective evaluations of comfort sensation, no plots such as those for thermal sensation are presented because at no time during the tests did any of the subjects indicate anything other than "comfortable" when questioned.

COMPUTER SIMULATION OF MAN, THE LCG, AND THE CONTROLLER

This section of the report presents the development of a computer simulation of the experimental procedures described in the previous sections. The computer simulation has been written in the IBM language entitled "Continuous System Modeling Program" (CSMP) (ref. 16).

An essential element of this control system simulation is a biothermal model of man. The starting point for the model was developed by Winton (refs. 17 and 18). A significant feature of Winton's model is the active control of the standard thermoregulatory processes of sweating, vasodilation, and shivering. The output of the model which directly affects the LCG temperature control loop is water loss. This includes loss through evaporated sweat, as allowed for by Winton's model, and respiratory water loss, which has been included in the development of a revised biothermal model of man.

The principal features of the experimental control loop which are considered in the computer simulation have already been introduced in figure 3. Briefly, these include: a) measurement of the dew point of the ventilating air at the outlet of a loose-fitting outer garment (AVG) encapsulating the subject; b) the control logic which prescribes the inlet water temperature to a liquid-cooled garment (LCG) as a function of a subject's evaporative water loss rate; c) a proportional valve which responds to the controller to provide the prescribed water temperature; and d) the liquid-cooled garment.

Interactions between the model and the environment include heat transfer from the skin to the LCG, from the skin to the ventilating air, and from the body core to the inspired air. Additionally, mass transfer (and consequently, heat transfer as latent heat) is included for evaporated sweat and respiratory water loss. All the exchange coefficients associated with these interactions have been approximated based on standard heat and mass transfer analyses of the data generated in the related experimental program.

The underlying strength and uniqueness of the current computer simulation development is the availability of closely related and extensive experimental data with which to compare and improve the computer model. The process of adjusting the various parameters in the model (consistent with the state-of-the-art knowledge concerning these parameters) in order to bring the model into closer agreement with the experimental data has been beneficial in two important respects. First, the quantitative accuracy of the model has been greatly improved, and second, the interpretation and understanding of the physical processes affecting the experimental results have been enhanced.

In the following paragraphs, a brief description of Winton's biothermal model of man is presented, followed by a discussion of the essential elements of difference between Winton's model and the revised biothermal model developed in the present study. Next, the LCG control loop and its computer simulation are presented and the procedures used to "tune" the model are described. Finally, representative results from the computer simulation are compared with experimental data.

Winton's Biothermal Model

The basic biothermal model of man developed by Winton is shown in analogous electrical circuit form in figure 25. Winton dealt almost exclusively with a two-layer model (core and skin) as opposed to a three-layer model (core, muscle, and skin) because of uncertainties in evaluating the three heat conductances required with the three-layer model. The specific correlation between heat transfer concepts and their analogous electrical circuit parameters are as follows: temperature corresponds to electrical potential, heat flow rate to electrical current, heat conductance to electrical conductance, and heat capacity to electrical capacitance.

A major contribution of Winton's model was the inclusion of active control over the thermoregulatory mechanisms of sweating, vasodilation, and shivering. The control signal (ERR) actuating his thermoregulatory mechanisms has both a core and a skin temperature contribution. The core contribution is simply the difference between the core temperature T_C and a reference temperature T_{REF}, multiplied by a suitable gain. The values selected by Winton for T_{REF} and the gain were 37.1° C and 1.0, respectively. For the skin contribution Winton included inputs based on both the skin temperature and its time derivative using a lead-lag circuit whose transfer coefficient is shown in figure 25. The skin feedback signal was zero for values of T_S greater than 33° C, and the skin gain was somewhat arbitrarily set at 0.025. Winton's treatment of the core and skin feedback signals, as well as the functional dependencies of the thermoregulatory mechanisms upon his total feedback signal, is based on the work of Benzinger (ref. 19). Winton based the contribution of the time derivative portion of the skin feedback signal solely upon the metabolic (shivering) response to step transients in skin temperature and then extrapolated this effect to the entire thermoregulatory process. In developing the revised biothermal model for the present study, the value of this contribution was considered minimal and therefore eliminated.

In the condensation of Winton's dissertation (ref. 18) and in most of the dissertation itself (ref. 17), the concept considered was the two-layer model of figure 25. However, when dealing with the imposed condition of exercise as the primary driving force in the model (as in the current simulation), Winton recognized the importance of expanding to a three-layer model which included the muscle. The muscle then became the source of metabolic heat during exercise. Winton's three-layer model is shown in figure 26 and the functional relationships selected for the three conductances required are displayed in figure 27. By Winton's statement, the values shown in figure 27 for G_{V1}, G_{V2}, and G_{V3} are gross approximations because of a dearth of related data.

Winton checked the validity of his model against the imposed conditions of hot and cold environments, humidity, exercise, ice ingestion, and fever. In all cases the model's response was favorable and encouraging, but actual comparisons with experimental data were limited and were more qualitative than quantitative in nature. Accordingly, Winton's model was selected as the starting point for the present computer model development, with revisions being dictated as a result of comparisons with the body of data made available in the related experimental program.

Revised Biothermal Model

In the initial stages of development of the present computer simulation of the entire LCG control loop, Winton's two-layer biothermal model was employed precisely. However, it quickly became obvious that a three-layer model would be necessary for quantitative comparisons between simulation and experiment. If the total exercise metabolic heat was introduced directly into the core (as required for the two-layer model), the computer simulation prediction of core temperature T_C increased much too early in comparison with the experimental data.

The basic structure of the revised biothermal model which has evolved is shown schematically in figure 28; the blocks of this diagram are numbered to correspond to sections of the CSMP program (presented in appendix A) in which details of the functions noted in the blocks are given. Many aspects of the revised model are directly comparable to Winton's model and will not be discussed further; significant changes or new features of the revised model are discussed in the following paragraphs.

Vasomotor control functions (G_{V1}, G_{V2}, G_{V3})– These three quantities were initially prescribed as given by Winton. However, comparisons between simulation and experimental data (with physiological justification based on refs. 20, 21, and 22) have suggested that the functions G_{V1} and G_{V3} be additionally dependent on exercise rate. Many adjustments of these functions were made in the course of tuning the model.

Feedback signal (ERR)– ERR has been made dependent on the core and skin temperatures T_C and T_S, but not on the time derivative of T_S as was the case for Winton's model. This change was made because severe instabilities in the simulation results were traced to the contribution of the time derivative. This change reduced the number of total system parameters by one, and is justified by Winton's observation concerning the general uncertainty surrounding the core and skin feedback contributions. To offset the diminished skin feedback, the skin gain was increased to 0.05.

Reference temperature variation (DT_{REF})– The accuracy of the simulation was improved by reducing the reference temperature by 0.2° C during exercise. Support for such a reduction is offered by Hammel (ref. 23).

Basal metabolism (M_{BAS})– The basal metabolism was set at 67.5 W, based on the average of oxygen consumption measurements for two of the test subjects. The total M_{BAS} was divided in the ratio of 75 percent to 25 percent between the core and muscle, respectively, as was done by Winton.

Exercise metabolism (M_{EX})– Values of this parameter were also established based on the average of oxygen consumption measurements for two of the test subjects. The following equations relating exercise metabolism and treadmill speed were developed by least-squares curve-fitting techniques:

$$M_{EX} = 20.3 + 248\ V_{TM} \qquad [\text{for } V_{TM} \leqslant 0.585] \tag{9}$$

$$M_{EX} = 125 + 98.3(V_{TM})^2 \qquad [\text{for } V_{TM} > 0.585] \tag{10}$$

For $V_{TM} = 0$, 20.3 W represents the increase in exercise metabolism measured for the subjects standing on the treadmill, as opposed to sitting. In developing the computer simulation program for the revised model, 90 percent of the exercise metabolism was arbitrarily assumed to take place in the muscle layer and 10 percent in the core layer of the model. This assumption is in contrast to that of Winton who assigned all the exercise metabolism to the muscle layer of his three-layer model. In arriving at the 90 percent: 10 percent division, it was recognized that although most of the metabolism associated with exercise occurs in the muscle masses, the activity of many of the organs in the body core also increases with exercise; furthermore, the assignment of 10 percent of the increased heat production to the core kept the core temperature T_C from dropping excessively immediately after the start of exercise as a result of increased core heat loss through increased respiration.

Pulmonary ventilation rate (V_R)– As in the cases of basal metabolism and exercise metabolism, pulmonary ventilation rate was related to oxygen uptake through measurements for two of the three test subjects during exercise. The following expression for pulmonary ventilation rate in terms of total metabolic rate was developed:

$$V_R = 2.28 + 0.045\ M_{TOTAL} \tag{11}$$

Pulmonary ventilation rate as expressed by this equation is consistent with the results presented by Astrand and Rodahl in reference 24.

Latent heat transfer through respiration (H_{ER})– The rate of respiratory heat loss through evaporation H_{ER} and its water vapor flow rate equivalent W_{ER} were evaluated based on the assumption that the respiratory air entered the body with a vapor pressure corresponding to that of the supply air to the AVG and exited as saturated air at the core temperature. The addition of this feature to the biothermal model is quite important in view of the significant effect shown for W_{ER} in the exercise tests.

Sensible heat transfer through respiration (H_{SENSR})– The rate of sensible heat transferred through respiration is small, but was included in the revised biothermal man-model for completeness. It is computed based on the assumption that the respiratory air enters the body at the rate V_R and a temperature T_{AI} corresponding to that of the supply air to the air ventilation garment and exits at core temperature T_C.

Sweat rate (S_{R1})– Although the prediction of sweat output from a human subject is of current interest, it is also uncertain. Not only is there quantitative disagreement among various investigators, there is even a lack of concensus as to the proper functional dependency of sweat rate upon physiological parameters. For example, Winton followed the work of Benzinger (ref. 19) by considering sweat rate to be a function of both skin and core temperature through his defined error signal ERR. In so doing, he specified the contribution of core temperature to be forty times more effective than that of skin temperature by assigning gain factors of 1.0 and 0.025, respectively, for his calculations of sweat rate. Stolwijk et al. (ref. 25) computed sweat rate by the following two methods: 1) as a linear function of metabolic rate and ambient air temperature; and 2) as a linear function of rectal and skin temperatures with a ratio of gain factors of 7 to 1, respectively, for the two temperatures. Stolwijk et al. proved their two methods to be compatible by showing (for their unclothed subjects exercising under steady state conditions) that skin temperature was a linear function of ambient temperature and that rectal temperature was a linear function of metabolism. A basic problem associated with using the methods of Stolwijk et al. in the current nonsteady state simulation is a difference in the sweat rates predicted by the two methods for the conditions associated with a step increase in exercise rate. This difference occurs because the rise in rectal temperature significantly lags behind the onset of increased metabolism.

The absence of a generally acceptable method of sweat rate prediction was taken as justification in the present simulation to combine the above approaches into a hybrid method whose results agree well with the experimental data. The resultant method uses two prediction equations. One is a function of the temperature feedback signal ERR and is simply a modified version of Winton's method, while the other expresses sweat rate as a linear function of metabolism and skin temperature in a manner comparable to that of Stolwijk. The CSMP simulation actually uses the smaller of these two predictions at any instant.

Latent heat transfer from skin (H_{ES})– Evaluation of the rate at which sweat is actually evaporated from the skin (W_{ES}) is a complex mass transfer problem, inasmuch as it involves consideration of air flow over an irregular shape that is partially covered by an absorbent garment. The garment adds complexity in that it is maintained (by the LCG cooling water) at a temperature different from the skin temperature and introduces an effective resistance and capacitance which affects the transfer of water vapor from that portion of the skin which it covers. Consequently, the following approximate procedure was employed to predict W_{ES} and its heat equivalent H_{ES}.

Because of mass transfer rate restrictions, W_{ES} is considered to be limited to W_{ESMAX} at high rates, while at low rates it is equal to sweat rate S_{R1}. W_{ESMAX} has been set equal to 156 g/hr based on the maximum outlet air dew point measured during the 2 m/sec exercise regime of the experimental investigation; W_{ES} reached this maximum and leveled off even though exercise continued and the rectal temperature kept rising. When there is no accumulated sweat S_{ACUM} in the LCG (computed as the time integral of the difference between S_{R1} and W_{ES}), is set equal to S_{R1}. When sweat has accumulated, W_{ES} is expressed by the equation

$$W_{ES} = (A_{WET})(W_{ESMAX}) + (1 - A_{WET})(S_{R1}) \quad (12)$$

in which A_{WET}, the fractional wetted area of the LCG, is computed as the ratio of current accumulated sweat S_{ACUM} to the maximum value so far attained by S_{ACUM} during the simulation. Thus, as S_{ACUM} increases during exercise, A_{WET} remains equal to 1.0; after exercise is terminated and S_{ACUM} decreases, A_{WET} is equal to the ratio of S_{ACUM} to S_{ACMAX} and decreases accordingly.

The methods used to predict S_{R1} and W_{ES} in the present simulation are open to question and the development of improved methods represents a major potential area of refinement of the simulation. Consequently, simulation results presented later in the paper have been computed in two manners, one entitled "closed loop" and the other "open loop." The closed-loop simulation employs the methods described above for predicting S_{R1} and W_{ES}, while the open-loop simulation avoids these two difficult predictions by utilizing actual rates of sweat evaporation as determined from the experimental hygrometer data.

Heat transfer from skin to LCG (H_{STL})– The predominant mode of heat transfer from the skin, especially at the higher metabolic rates, is by conduction to the LCG and is expressed as

$$H_{STL} = (T_S - T_{LAVE})(EX_{STL}) \quad (13)$$

The heat exchange coefficient EX_{STL} was initially estimated from an examination of the experimental data and was later refined to include contributions associated with exercise rate and accumulated sweat.

Heat transfer from skin to ventilating air (H_{STA})– Computation of this quantity is analogous to the foregoing:

$$H_{STA} = (T_S - T_{AAVE})(EX_{STA}) \quad (14)$$

Because of the relatively small contribution of H_{STA} in comparison with H_{STL}, the exchange coefficient EX_{STA} – 4.4 W/°C – as estimated from the experimental data was used with no attempt at further refinement.

Heat capacitances (C_C, C_M, C_S)– Initially these capacitances were prescribed exactly as Winton had done in his three-layer model. However, in order to reduce the amplitude of the oscillations in some of the simulation results for skin temperature (which is an extremely sensitive parameter at the higher metabolic rates because of the effect of the large heat flux through the skin combined with its low heat capacity), the skin heat capacitance C_S was doubled. This resulted in a skin heat capacitance equal to approximately 10 percent of the total body heat capacitance; however, the increase can be justified in view of the general uncertainty of the precise boundary of the skin.

LCG Control Loop

The overall control loop as considered for the present computer simulation is illustrated in figure 3. As mentioned before, the numbers in the blocks in this figure refer to sections in the CSMP

program which is included in appendix A. Inputs to the system include ventilating air at a fixed volume flow rate A_{FR} and with prescribed constant values of inlet temperature T_{AI} and dew point T_{DPI}. The volume flow rate of water to the LCG, W_{FR}, is also fixed, while its inlet temperature T_{LI} is the primary controlled quantity in the simulation.

The majority of the elements comprising the control system were considered to be first order components in describing their mathematical function. This approach was employed for the sake of simplicity and its validity was substantiated experimentally. The experiments involved isolating the input and output of selected elements, imposing a step change to the input, and measuring the resulting output. This procedure established the delay and rise times for the selected elements as required for their first order descriptions. (A summary of these experimental determinations is included in appendix C.) Elements of the control system so considered were the ventilating outer garment, the hygrometer and its air supply line, the LCG controller and the controlled proportional valve, the water supply line from the proportional valve to the LCG inlet, and the LCG itself from inlet to outlet.

The computer simulation includes a heat balance for the LCG which yields the value of outlet water temperature T_{LO} and, in turn, the total heat transfer rate to the LCG, H_{LCG}. This balance prescribes heat transfer between the skin and the LCG, and between the ventilating air and the LCG according to equations (13) and (15).

$$H_{ATL} = EX_{ATL}(T_{AAVE} - T_{LAVE}) \tag{15}$$

The value of T_{LAVE} at any instant is based on simulation values of T_{LI} and T_{LO} computed for the previous second. This procedure is required because T_{LAVE} and T_{LO} are interdependent. The described procedure solved the classical loop problem, and similar techniques were employed to compute T_{AAVE} and P_{WAVE}. (Appendix B presents details of the evaluation of the exchange coefficients EX_{STL} and EX_{ATL}, as well as EX_{STA} and EX_{AVG} which are introduced in the following paragraphs.)

In a manner comparable to that described above, the computer simulation performs a continuous heat balance for the air passing through the air ventilation garment, thereby determining the outlet air temperature T_{AO} and the total sensible heat transfer rate to the ventilating air, H_{ASENS}. Equations (14) and (16) were used to express the heat transfer rates from the skin to the ventilating air and from the ventilating air through the air vent garment wall to the ambient environment:

$$H_L = EX_{AVG}(T_{AAVE} - T_G) \tag{16}$$

An additional component considered in the overall heat balance for the ventilating air was the rate of sensible heat transfer to the respired air which was expressed by the equation:

$$H_{SENSR} = 0.0188(V_R)\,(T_C - T_{AI}) \tag{17}$$

Finally, a water vapor balance for the ventilating air was continuously computed by the CSMP program. This balance specifies that the water vapor mass flow rate, WV_{OG}, leaving the air vent garment is equal to the entering rate plus the additions from evaporated sweat and respiration:

$$WV_{OG} = WV_{IG} + W_{ES} + W_{ER} \tag{18}$$

Knowing WV_{OG} permits the computation of the total latent heat transer rate to the air, H_{ALAT}, and the difference between the instantaneous water vapor mass flow rate from the air vent garment and its basal value for a resting subject provides the primary signal DWL_{ID} for the LCG control loop simulation:

$$DWL_{ID} = WV_{OG} - WV_{OGB} \tag{19}$$

This relationship is illustrated in figure 7. The algorithm prescribing the desired cooling water temperature from the mixing valve T_{SET} as a function of the incremental rate of water vapor loss DWL_{ID} is:

$$T_{SET} = 32.2 - 0.1325\ DWL_{ID} \tag{20}$$

The actual temperature of the water entering the LCG is less than T_{SET} due to losses in the supply line, and this temperature T_{LI} for the computer simulation program is expressed by the following equation which was determined based on data from the experimental program:

$$T_{LI} = 2.5348 + 0.921(T_{SET}) \tag{21}$$

Adjustment of Model Parameters

The process of adjusting the CSMP model to bring it into close agreement with the experimental data was an inexact process at best; heavy reliance was placed on intuition. Certain criteria were basic to the adjustment process and three of the most important considerations were the following:

1. The starting point for the adjustment of all parameters in the man model, exclusive of the new features described previously for the revised biothermal model, was Winton's three-layer model.

2. All adjustments of physiological or physical parameters in the model were constrained within the bounds of current knowledge concerning the parameters.

3. The majority of the model tuning was done for the 2 m/sec simulation – activity schedule IV – utilizing average results from test number 4. This was the most critical situation inasmuch as the prime driving force, the exercise metabolic rate M_{EX},was larger than for the other single step tests. Additionally, the data for the 2 m/sec simulation were less complex and more easily interpreted than were the data for activity schedules V and VI, the other two schedules with high exercise metabolic rates.

An examination of the parameters of the computer simulation and the experimental investigation reveals that there are six variables – T_C, T_S, T_{LI}, H_{ALAT}, H_{LCG}, H_{ASENS} – that are directly and separately comparable between the simulation results and the experimental data. It was advantageous in some instances to assign priorities to certain of the experimental variables when making adjustments in the model. For instance, T_C from the experiments was given greater credence than

T_S because of the greater confidence placed in the accuracy of measurement and interpretation of T_C; T_C was derived from a single, reliable, rectal thermistor, while the experimental T_S was based on an average of the six skin thermistor readings whose individual accuracies could be influenced by their environment, that is, exposure to ventilating air or contact by LCG tubes. Likewise, consideration of H_{LCG} was given priority over H_{ASENS} because of its greater magnitude during the exercise period.

It became apparent during initial considerations of the complete model that it would be advantageous to isolate segments of the model and modify them independently based on related experimental data rather than to attempt to improve the entire model at one time. The inner portion of the model was the first portion to be isolated. This isolation was effected by reading into the computer the experimental values for average skin temperature T_S, thereby defining realistic boundary conditions with which the core and the muscle parameters of the model interfaced. The primary experimental parameter with which the simulation results were compared during this particular model segmentation was core temperature T_C; additionally, muscle temperatures from the simulation were compared qualitatively with available data from the literature.

The first step of the optimization effort led to the determination of the values of the conductances G_{V1}, G_{V2}, and G_{V3} as listed in the CSMP program (appendix A), plus the introduction of a variable reference temperature DT_{REF} into the man model. It was mentioned earlier that G_{V1} and G_{V3} were considered to be dependent on exercise metabolism as well as on the total feedback signal ERR; these considerations met an indicated need for greater magnitudes for these conductances immediately after the start of exercise than could be attained through dependency on ERR alone. The variable reference temperature was introduced to account for an observed decrease in rectal temperature from 37.3° C to 37.1° C during the initial 20-minute rest period of the experimental activity schedules. The use of Winton's suggested constant reference temperature of 37.1° C would have resulted in an appreciable negative ERR during the rest period, giving rise to sweating and vasodilation in the model. Alternatively, the use of a constant 37.3° C was found to delay the onset of sweating after the beginning of exercise. The incorporation of 0.2° C reduction of reference temperature during the rest period for the simulation, as measured during the experiments, prevented these discrepancies.

Conditions during the initial 20-minute rest period of the experiments were also utilized in arriving at base levels (when ERR and M_{EX} equal zero) for G_{V1}, G_{V2}, and G_{V3}; they were determined from heat balance considerations of the entire man model such that reasonable values of muscle temperature T_M were correlated with the variable T_C (37.3° C to 37.1° C), while skin temperature T_S was constant at 33.5° C.

For the second phase of the optimization effort, the skin temperatures T_S which were read into the computer program for the first phase were retained and experimental values were read in for the inlet temperature to the LCG T_{LI}. This procedure effectively isolated the heat exchange process between the skin and the LCG and permitted the refinement of the original approximation of the related heat exchange coefficient EX_{STL} (see appendix B) through comparison of simulation and experimental results for H_{LCG}. As a result of this analysis, it was found that EX_{STL} should be about 8.5 W/°C during the initial rest period, should increase abruptly by about 9 W/°C at the onset of exercise, then continue to rise gradually during exercise (for an increase of about 3 to 4 W/°C for the 2 m/sec simulation), and finally decrease gradually to the initial value during the final resting

period. The physical explanation which is proposed to account for these variations is that the heat exchange coefficient EX_{STL} is comprised of a base value EX_{STLR}, an exercise component EX_{STLX}, and an accumulated sweat component EX_{STLA}. The exercise component is attributed to the more intimate contact between the subject's skin and the heat exchange tubes of the LCG during exercise than during rest; the accumulated sweat component is attributed to the increased conduction of heat from the skin to the LCG due to the moisture which builds up during the exercise period.

For the final segmentation of the simulation model, values were read into the program for the rate of water evaporation from the skin W_{ES}, while all other parameters of the complete model were computed normally. Values of W_{ES} were obtained by subtracting respiratory water loss W_{ER} from the total water loss which was computed based on the total latent heat loss to the ventilating air H_{ALAT}. The mode of simulation represented by this final segmentation is the mode referred to previously as "open loop," and it permitted adjustments of the portions of the model dealing with W_{ES} and sweat rate S_{R1}.

With all refinements incorporated from the segmentations of the program, the final adjusted computer model was run in the mode designated as "closed loop." The results of both the open and closed loop simulations are presented in the following paragraphs.

Model Results and Discussion

Computer simulation results are presented for comparison with experimental data from tests 2, 4, and 6 (activity schedules II, IV, and VI, fig. 9). Test 2 included a moderate (1 m/sec) single step exercise regime, test 4 included a strenuous (2 m/sec) single step exercise regime, and test 6 included a representative complex exercise schedule. Results for the three tests are shown in figures 29, 30, and 31, respectively. The parameters plotted in the figures are T_{LI}, T_S, ΔT_C, H_{ALAT}, H_{LCG}, and H_{TOTAL}; results are included for both open loop and closed loop simulations. The averaged experimental results for the three test subjects are also shown.

Both the open and closed loop simulation results are good approximations to the experimental data, particularly in view of the complex nature of the physical and physiological systems which have been simulated. The general superiority of the open loop simulation, which is evident in figures 29-31, was expected since the open loop method utilized experimental values of sweat rate and evaporative water loss, while the closed loop method employed an analytical process to predict these two variables. The refinement of the analytical prediction of these two parameters was mentioned earlier as a significant area for improvement in the future development of the revised biothermal model of man.

Two additional comments, pertaining to the open loop simulation results, but generally applicable to either the open or closed loop simulations, suggest additional areas of possible improvement of the models:

1. Core temperature simulations T_C for tests 2 and 4 follow the experimental data quite well, except that they show too rapid a decay of temperature after termination of exercise, and the simulation values, particularly for test 2, are slightly low at the end of the exercise period.

2. Simulation results for T_C for test 6 (fig. 31) are qualitatively consistent with the experimental data but are about 0.3° C to 0.4° C high during the last half of the test period. The reason for this is not evident; the discrepancy is especially puzzling in view of the close agreement between the simulation and experimental skin temperatures T_S, and the fact that the simulation values for the heat transfer rates H_{LCG} and H_{TOTAL} generally exceed the corresponding experimental values.

The simulation results for T_S computed by the open loop method are quite accurate for all three tests. This accuracy is particularly remarkable because of the sensitivity of this parameter to the combined effects of the generally high heat flux rate and low heat capacitance for the skin, as was discussed previously. The open loop computations for H_{LCG} and H_{TOTAL} are also fairly consistent with the test data; for tests 2 and 4 (figs. 29 and 30), the equilibrium values of H_{TOTAL} reached toward the end of the exercise periods agree well with the metabolic rates prescribed in the simulation and based on the data of figure 10, where metabolic rate is shown as a function of treadmill speed.

CONCLUDING REMARKS

The physiological and subjective comfort data generated in the present experimental investigation showed that the temperature of a liquid-cooled garment of the type worn by the Apollo astronauts could be effectively regulated by an automatic temperature controller utilizing evaporative water loss rate as the primary measured variable. Limitations of the controller's effectiveness were apparent only at high exercise rates – of the order of 2 m/sec – for the level treadmill used, corresponding to an exercise metabolic rate of 500-600 W. At this work rate, the subjects secreted more sweat than could be evaporated so that the total latent heat transfer rate to the ventilating air reached a maximum while the core temperature continued to rise. After termination of exercise in these cases, the evaporation of residual moisture resulted in a somewhat low liquid-cooled garment temperature and a correspondingly low skin temperature and calculated mean body temperature at the end of the test period. Even with these limitations, however, none of the three test subjects expressed unusual thermal discomfort during the tests.

Two styles of liquid-cooled garments were utilized. One was identical to the type worn by the Apollo astronauts; the other was also identical in design and fabrication, except for the addition of head- and neck-cooling provisions. The added cooling capability was quite effective in reducing the active sweat rate of the subjects and as a result, the liquid coolant temperature required was not as low as with the Apollo-type garment; skin and mean body temperatures were therefore not as low, and the modified garment was more comfortable.

In the analytical portion of the study, a biothermal model was developed (by extension and revision of Winton's existing model) of the human thermoregulatory system in conjunction with a liquid-cooled garment and automatic temperature controller as used in the experimental investigation. All heat transfer interactions between the man, the liquid-cooled garment, the air ventilation garment, and the environment were simulated and appropriate heat transfer coefficients were defined to permit computer simulations of the same exercise regimes as were included in the experimental investigation. The simulation results were considered to be good approximations of

the experimental data, particularly in the cases of skin temperature, heat transfer rate to the liquid-cooled garment, and the total heat transfer rate (which included the total sensible and latent heat transfer rates to the ventilating air, the total heat transfer rate to the liquid-cooled garment, and the heat loss rate through the air ventilation garment). The model substantiated the impression gained from the experiments that the thermoregulatory control of sweating, including its production and subsequent evaporation through the LCG, is an extremely complex process; to understand fully the thermal responses of a man wearing an LCG, more investigation is necessary. Significant areas identified for future improvement of the model were in the analytical prediction of sweat rate, total evaporative water loss rate, and core temperature variation during complex exercise schedules.

Ames Research Center
National Aeronautics and Space Administration
Moffett Field, Calif. 94035, December 8, 1972

APPENDIX A

CONTINUOUS SYSTEM MODELING PROGRAM FOR THE REVISED BIOTHERMAL MODEL OF MAN

```
. . . $JOB LIST, 0071
. . . $ASSIGN 5=CR, 6= LP1
. . . $EXECUTE LIST
```

```
LABEL WINTON MODEL WITH LCG AND CONTROLLER ADDED
*  THIS MACRO GIVES PSAT OF H20 IN MM HG AS FCN OF TSAT IN DEG C
MACRO OUT = PSAT (A, B, C, D, INPUT)
T = INPUT +273.16
U = 647.27–T
Z1 = (U/T) * ( (A+B*U+C*U** 3) / (1.0+D*U) )
OUT = (218.167 / (10.**Z1) )* (760.0)
ENDMAC
*THERMAL ANALOG OF BODY
EXSTLR = 8.5
EXSTLX = 9.0*YEX2
EXSTLA = .0222*SACUM
EXSTL = EXSTLR+EXSTLX+EXSTLA
HCTS=GV2* (TC-TS)
HCTM=GV1*(TC-TM)
HTCNET = -HCTS-HCTM-HSENSR-HER+MC
TC=INTGRL (ICTC,HTCNET/CC)
HMTS=GV3* (TM-TS)
HTMNET= -HMTS+HCTM+MM
TM=INTGRL (ICTM,HTMNET/CM)
HSTL=EXSTL* (TS-TLAVE)
HSTA=EXSTA* (TS-TAAVE)
HTSNET=HMTS+HCTS-HES-HSTL-HSTA
TS=INTGRL (ICTS,HTSNET/CS)
* FEEDBACK STRUCTURE
*  NOTE 18
SLIM=COMPAR (33.0, TS)
SKDEL=TS-33.0
W=SKDEL*SLIM
FBS=GNS*W
FBC=GNC*TC
```

```
* NOTE 1
DTREF = 0.2*YEX2
TREF = 37.3-DTREF
TRA = TREF-FBS
ERR = TRA-FBC
* CONTROLLER FUNCTIONS
* NOTE 5
* FOR CORE TO MUSCLE CONDUCTANCE (WATTS/DEG C)
GV1S = .1 * MEX2
GV1P = REALPL (0.0, 30., GV1S)
GV1ERR = AFGEN (CURVE 7, ERR)
GV1 = GV1P + GV1 ERR +30.0
* NOTE 4
* FOR CORE TO SKIN CONDUCTANCE (WATTS/DEG C)
GV2 = AFGEN (CURVE 5, ERR)
* NOTE 3
* FOR MUSCLE TO SKIN CONDUCTANCE (WATTS/DEG C)
GV3S = .0452*MEX
GV3P = REALPL (0.0, 120., GV3S)
GV3 = 5.5 + GV3P
* NOTE 17
* FOR METABOLIC RATES (WATTS)
MC = .75*MBAS+.10* (MEX+MSH)
MM = .25*MBAS+.90* (MEX+MSH)
* NOTE 6
MSH=AFGEN (CURVE 3, ERR)
* SECTION FOR DESCRIBING MEX, EXERCISE PROFILE NUMBER 4
TITLE 2.0 M/SEC, 20 TO 50 MIN, REST FROM 50 TO 75 MIN
VTM = 1.97
YEX1A = PULSE (20., (TIME-1180.) * (1200. -TIME))
YEX1B = PULSE (20., (TIME-3000.) * (3020. -TIME))
YEX1 = YEX1A + YEX1B
MEX1 = FCNSW (YEX1, 0., 0., 20.3)
YEX2 = PULSE (1800., (TIME-1200.) * (3000.-TIME))
MEXT = 125. +98.3 * (VTM ** 2)
MEX2 = FCNSW (YEX2, 0., 0., MEXT)
MEX = MEX1 + MEX2
M TOTAL = MBAS+MEX1+MEX2
* NOTE 9
* FOR VENTILATION RATE (L/MIN) AS FCN OF MTOTAL
VR = 2.28 + .045 * (MTOTAL)
* NOTE 15
```

```
* FOR SENSIBLE RESPIRATORY HEAT LOSS (WATTS)
HSENSR = .0188 * VR * (TC-TAI)
* FOR VAPOR PRESSURE (MM HG) OF AIR ENTERING SUIT
PWI = PSAT (A, B, C, D, TDPI)
* NOTE 12
* FOR VAPOR PRESSURE (MM HG) OF EXPIRED AIR
PWC = PSAT (A, B, C, D, TC)
* NOTE 13
* FOR RESPIRATORY WATER LOSS (GM/HR)
WER = .0556 * VR * (PWC-PWI)
WERTOT = INTGRL (0.0, WER/3600.)
* NOTE 14
* FOR EVAPORATIVE RESPIRATORY HEAT LOSS (WATTS)
HER = .678 * WER
* NOTE 11
* FOR VAPOR PRESSURE (MM HG) AT SKIN TEMPERATURE
PWS = PSAT (A, B, C, D, TS)
* FOR WATER VAPOR RATE (GM/HR) INTO SUIT
WVIG = .0594 * PWI * AFR
* FOR DELAYED VAPOR PRESSURE (MM HG) OF AIR LEAVING SUIT
PWOD1 = 5.75
PWOD2 = DELAY (10, 1., PWO)
YPWO = STEP (1.0)
PWOD = FCNSW (YPWO, PWOD1, PWOD1, PWOD2)
* FOR AVERAGE VAPOR PRESSURE (MM HG) IN SUIT
PWAVE = (PWI + PWOD)/2.0
* NOTE 10
* FOR MAX EVAP RATE FROM SKIN (GM/HR).
WESMAX = 156.
* NOTE 2
* FOR PHYSIOLOGICAL SWEAT RATE (GM/HR)
SR1A= 1.0 * MTOTAL + 49.8 * TS-1700.
SR1B = SR1A -18.6
SR1C = INSW (SR1B, 18.6, SR1A)
SR1MET = REALPL (18.6, 50., SR1C)
SR1MAX = AFGEN (CURVE 1, ERR)
WEVER = SR1MAX-SR1MET
SR1 = INSW (WEVER, SR1MAX, SR1MET)
STOTAL = INTGRL (0.0, SR1/3600.)
WLTOT = STOTAL + WERTOT
* NOTE 7
* SWEAT ACCUMULATOR SECTION.
```

```
WESD1 = SR1
WESD2 = DELAY (10, 1.0, WESCMP)
YWES = STEP (1.0)
WESD = FCNSW (YWES, WESD1, WESD1, WESD2)
SACR1 = SR1-WESD
ISACR = COMPAR (SACR1, 0.0)
SACUD1 = 0.0
SACUD2 = DELAY (10, 1.0, SACUM)
YSACUM = STEP (1.0)
SACUMD = FCNSW (YSACUM, SACUD1, SACUD1, SACUD2)
SACRP = SACR1
SACRN = FCNSW (SACUMD, 0.0, 0.0, SACR1)
SACR = FCNSW (ISACR, SACRN, SACRN, SACRP)
SACUM = INTGRL (0.0, SACR/3600.)
SACMAX = ZHOLD (ISACR, SACUM)
ISACUM = COMPAR (SACUM, 1.0)
SR2 = FCNSW (ISACUM, SR1, SR1, 20000.)
* NOTE 8
* FOR ACTUAL EVAP RATE FOR SKIN (GM/HR)
WESCAL = LIMIT (0.0, WESMAX, SR2)
RATIO = SACUM/(SACMAX + 0.0001)
AWET = LIMIT (0.0, 1.0, RATIO)
WESNRT = WESCAL * AWET +SR1 * (1. -AWET)
WES = REALPL (18.6, 50.0, WESNRT)
* NOTE 16
* FOR EVAPORATIVE HEAT LOSS FROM SKIN (WATTS)
HES = .678 * WES
* NOTE 20
* FOR WATER VAPOR RATE (GM/HR) OUT OF SUIT
WVOGS = WVIG + WER + WES
WVOSD1 = WVOGS
WVOSD2 = DELAY ( 17, 1.7 , WVOGS)
YWVOG = STEP (1.7)
WVOGSD = FCNSW (YWVOG, WVOSD1, WVOSD1, WVOSD2)
WVOG = REALPL (162.3, 28., WVOGSD)
* FOR VAPOR PRESSURE (MM HG) OF AIR LEAVING SUIT
PWO = WVOG/(.0594*AFR)
* FOR DELAYED TEMPERATURE (DEG C) OF AIR LEAVING SUIT
TAOD1 = TAI
TAOD2 = DELAY (10, 1., TAO)
YTAO = STEP (1.0)
TAOD = FCNSW (YTAO, TAOD1, TAOD1, TAOD2)
```

```
* FOR AVERAGE AIR TEMPERATURE (DEG C) IN SUIT
TAAVE = (TAI + TAOD)/2.0
* FOR DELAYED TEMPERATURE (DEG C) OF H2O ENTERING LCG
TLID1 = 32.2
TLID2 = DELAY (10, 1.0, TLI)
YTLI = STEP (1.0)
TLID = FCNSW (YTLI, TLID1, TLID1, TLID2)
* FOR DELAYED TEMPERATURE (DEG C) OF H2O LEAVING LCG
TLOD1 = 32.2
TLOD2 = DELAY (10, 1.0, TLO)
YTLO = STEP (1.0)
TLOD = FCNSW (YTLO, TLOD1, TLOD1, TLOD2)
* FOR AVERAGE H2O TEMPERATURE (DEG C) IN LCG
TLAVE = (TLOD + TLID)/2.0
* NOTE 20
* FOR TEMPERATURE (DEG C) OF AIR LEAVING SUIT
TAOS = TAI + HSTAN1 + HSENRN -HATLN - HLN
HSTAN1 = EXSTA * (TS-TAAVE)/(.01995 * AFR)
HSENRN = HSENSR/(.01995 * AFR)
HATLN = EXATL * (TAAVE-TLAVE)/(.01995 * AFR)
HLN = 1.0 * (.782 * (TAAVE-TG)-.2)
HL = .01995 * (.782*(TAAVE-TG) -.2) *AFR
TAOSD1 = TAOS
TAOSD2 = DELAY (17, 1.7, TAOS)
YTAOS = STEP (1.7)
TAOSD = FCNSW (YTAOS, TAOSD1, TAOSD1, TAOSD2)
TAO = REALPL (26.65, 28., TAOSD)
* FOR TOTAL SENSIBLE HEAT TO AIR (WATTS)
HASENS = .01995 * AFR * (TAO-TAI)
* NOTE 20
* FOR VAPOR PRESSURE (MM HG) INDICATED AT HYGROMETER
PWHD1 = PWO
PWHD2 = DELAY (44, 4.4, PWO)
YPWH = STEP (4.4)
PWHD = FCNSW (YPWH, PWHD1, PWHD1, PWHD2)
PWH = REALPL (5.68, 16.0, PWHD)
* NOTE 21
* FOR H20 LOSS (GM/HR) INDICATED AT ANALOG COMPUTER
WLID = .0594 * (PWH-PWI) * AFR
* FOR TOTAL LATENT HEAT TO AIR (WATTS)
HALAT = .678 * WLID
* FOR TEMPERATURE CALLED FOR BY CONTROL ALGORITHM
```

```
YTSET = COMPAR (WLID, 31.38)
DWLIDP = WLID -31.38
DWLID = FCNSW (YTSET, 0., 0., DWLIDP)
TSET = 32.2 -.1325 * DWLID
* NOTE 22
* FOR TEMPERATURE OF H2O DOWNSTREAM OF PROPORTIONAL VALVE
TVALD1 = TSET
TVALD2 = DELAY (11, 1.1, TSET)
YTVAL = STEP (1.1)
TVALD = FCNSW (YTVAL, TVALD1, TVALD1, TVALD2)
TVAL = REALPL (32.2, 3.8, TVALD)
* NOTE 23
* FOR TEMPERATURE OF H2O AT LCG INLET
TLISD1 = TVAL
TLISD2 = DELAY (110, 11.0, TVAL)
YTLIS = STEP (11.0)
TLISD = FCNSW (YTLIS, TLISD1, TLISD1, TLISD2)
TLILOS = REALPL (32.2, 15.0, TLISD)
TLI = 2.5438 + .921 * TLILOS
* FOR TEMPERATURE OF H2O AT LCG OUTLET
TLOS = TLI + HSTLN1 + HATLN1
HSTLN1 = EXSTL * (TS-TLAVE)/(69.94 * WFR)
HATLN1 = EXATL * (TAAVE-TLAVE)/(69.64 * WFR)
TLOSD1 = TLOS
TLOSD2 = DELAY (15, 1.5, TLOS)
YTLOS = STEP (1.5)
TLOSD = FCNSW (YTLOS, TLOSD1, TLOSD1, TLOSD2)
TLO = REALPL (32.2, 5.0, TLOSD)
* FOR TOTAL HEAT TO LCG (WATTS)
HLCG = 69. 64 * WFR * (TLO - TLI)
HTOTAL = HASENS + HL + HLCG + HALAT
DB1 = DEBUG (1,600.)
DB2 = DEBUG (1,1800.)
DB3 = DEBUG (1,3900.)
DB4 = DEBUG (1,4200.)
* DATA VALUES
* INITIAL TEMPERATURES FOR CORE, MUSCLE, AND SKIN
INCON ICTC = 37.3, ICTS = 33.5, ICTM = 36.7
* THERMAL CAPACITY OF CORE, MUSCLE, AND SKIN (WATT-SEC/DEG C)
PARAM CC = 147000., CM = 96400., CS = 25060.
* RELATED TO DETERMINING ERROR FOR HUMAN THERMAL CONTROL
PARAM GNS = 0.05, GNC = 1.0
```

```
* THERMAL EXCHANGE COEFFICIENTS (WATTS/DEG C)
PARAM  EXATL = 3.78, EXSTA = 4.4
* BASAL  METABOLIC RATE (WATTS)
PARAM  MBAS = 67.5
* GLOBE TEMPERATURE (DEG C)
PARAM  TG = 27.0
* CONDITION OF INLET AIR (DEG C)
PARAM  TAI = 20.0, TDPI = 0.0
* RELATED TO MACRO
PARAM A = 3.2437814, B = 5.86826E-03, C = 1.170238E-08, D = 2.187846E-03
* FLOW RATES (LITERS/MIN)
PARAM AFR = 481.0,  WFR = 1.89
* PHYSIOLOGICAL FUNCTION CURVES
AFGEN CURVE 1 = (-1000.0, 950.0, -1.6, 950.0, 0.0, 18.6, 1000.0, 18.6)
AFGEN CURVE 3 = (-1000.0, 0.0, 0.6, 0.0, 1.4, 343.0, 1000.0, 343.0)
AFGEN CURVE 5 = (-1000., 50., -1.84, 50.0, 0.0, 13.5, 1000., 13.5)
AFGEN CURVE 7 = (-1000., 350., -.9, 350., 0.0, 0.0, 1000., 0.0)
* PROGRAM RUNNING AND OUTPUT INFORMATION
METHOD RKSFX
TIMER DELT = 1.0, FINTIM = 4500., PRDEL = 60.0
PRINT TLI, TS, TC, TM, HALAT, HASENS, HLCG, ERR, . . .
HCTS, HCTM, HMTS, HTCNET, SR1MAX, SR1MET, WES, . . .
 SR1, HTOTAL, HL, WLTOT, SACMAX, SACUM, HSTL, HSTA
END
STOP
END JOB
```

APPENDIX B

EVALUATION OF HEAT TRANSFER COEFFICIENTS

Evaluation of four heat transfer coefficients (EX_{AVG}, EX_{ATL}, EX_{STL}, and EX_{STA}) is required for utilization of the accompanying CSMP program. The methods employed for these evaluations are presented in the following four sub-sections.

HEAT LOSS THROUGH THE AVG

In order to determine the total heat passing from the subject, both experimentally and for the computer simulations, it is necessary to evaluate the heat loss through the material of the air ventilation garment (AVG). This heat H_L can then be added to the measurable heat rejection modes (H_{ASENS}, H_{LCG}, and H_{ALAT}), thereby completing the total heat balance on the subject.

The heat loss through the AVG is considered to involve forced convection between the ventilating air and the interior of the AVG, conduction through the AVG material, and free convection on the outside of the AVG to the ambient surroundings. Accordingly, the driving force for the heat transfer process is the average air temperature in the air ventilation garment T_{AAVE} minus the ambient globe temperature T_G.

The overall heat transfer coefficient representative of the foregoing process was experimentally evaluated. This process was accomplished by placing a full-size manikin in the AVG and blowing air through the garment at the same rate selected for the regular experimental runs (481 liter/min), thereby simulating the desired flow conditions inside the AVG. Then the air inlet temperature T_{AI} was set to a particular value, equilibrium conditions were established as evidenced by the air outlet temperature T_{AO}, and the corresponding values of T_{AO} and T_G were recorded.

Repeating the procedure for several values of T_{AI}, both greater and less than T_G, yielded the results shown in figure 32. The ordinate of this figure is a measure of the heat gained (or lost) by the air in passing through the AVG, and the abscissa is the process driving force. Consequently, the slope of a line through the data points is directly related to the desired overall heat transfer coefficient. The equation of the line through the experimental points was determined by curve-fitting techniques to be:

$$T_{AO} - T_{AI} = 0.782(T_G - T_{AAVE}) + 0.2 \qquad (22)$$

The intercept value of 0.2° C included in the equation can be physically explained as the temperature rise resulting from viscous dissipation, occurring at the expense of a pressure drop in the ventilating air.

The following equation for heat transfer rate between the ventilating air and the ambient environment was obtained based on equation (22), the ventilating flow rate A_{FR}, and the density and specific heat of the ventilating air:

$$H_L = 0.01995[0.782(T_{AAVE} - T_G) - 0.2](A_{FR}) \quad (23)$$

HEAT TRANSFER RATE BETWEEN VENTILATING AIR AND THE LCG

Because several heat transfer processes occur simultaneously within the AVG under regular experimental conditions, it was necessary to devise an experimental arrangement which would permit separate evaluation of the individual heat transfer coefficients related to the various processes. Accordingly, the previously mentioned manikin was completely wrapped with an insulating foam rubber tape, dressed in the LCG, and placed in the AVG. The insulated manikin simulated an adiabatic body inside the AVG while retaining the proper air flow characteristics within the suit.

With water supplied to the LCG and ventilating air to the AVG, the simplified steady-state heat balance equation for the ventilating air is:

$$H_{ASENS} = EX_{ATL}(T_{LAVE} - T_{AAVE}) - H_L \quad (24)$$

This equation assumes that the ventilating air exchanges heat only with the LCG and across the AVG material with the ambient environment. Furthermore, the exchange with the LCG is assumed to have a driving force of T_{LAVE} minus T_{AAVE} and an exchange coefficient EX_{ATL}.

For a particular value of T_{LI}, the quantities H_{ASENS}, T_{LAVE}, and T_{AAVE} are measurable and H_L can be evaluated by equation 23. Consequently, a single test condition could provide the value of EX_{ATL}. However, several test conditions were selected in order to improve experimental accuracy; these data points are plotted in figure 33 in the form of $(H_{ASENS} + H_L)$ versus $(T_{LAVE} - T_{AAVE})$. The slope of the best straight-line fit to this data is the desired quantity EX_{ATL}; its value was found to be 3.78 W/°C.

HEAT TRANSFER RATE BETWEEN THE SKIN AND THE LCG

The value of the heat exchange coefficient EX_{STL} between the skin and the LCG was initially approximated as described below by an evaluation of selected data from the regular experimental program. Subsequently, the value of EX_{STL} so obtained was modified in the course of tuning the CSMP program.

Under steady state conditions during an experimental test run, the heat balance on the LCG appears as

$$H_{LCG} = H_{STL} + H_{ATL} \quad (25a)$$

Expressing the right-hand side in terms of exchange coefficients and corresponding temperature differences, this equation becomes:

$$H_{LCG} = EX_{STL}(T_S - T_{LAVE}) + EX_{ATL}(T_{AAVE} - T_{LAVE}) \quad (25b)$$

As determined above, the value of EX_{ATL} was 3.78 W/°C and all the other quantities in the equation, with the exception of EX_{STL}, were available from experimental data. Accordingly, a plot of $[H_{LCG} - EX_{ATL}(T_{AAVE} - T_{LAVE})]$ versus $(T_S - T_{LAVE})$ for the selected test conditions permits the establishment of a line having a slope equal to EX_{STL}.

Data considered to represent steady state conditions for each of the three test subjects were selected for use in the evaluation of EX_{STL}. In particular, the time-averaged values of H_{LCG}, T_S, T_{LAVE}, and T_{AAVE} for the exercise period from 61 to 65 minutes were used from tests 1, 2, 3, 7, 8, and 9; similary, data for the exercise period from 46 to 50 minutes were used from tests 4 and 10. The resulting data are plotted in figure 34; despite the scatter of the points, it is apparent that no obvious differences exist within the data which can be attributed to the type of LCG used, or to differences among the subjects. A reasonable equation for a curve passing through the origin could be developed for the data by curve-fitting techniques; however, a straight-line approximation was considered to be sufficiently accurate for the initial development of the CSMP program. The straight-line value selected for EX_{STL} was 21 W/°C. (In the process of refining the CSMP program, EX_{STL} was divided into resting, exercise, and sweat accumulation components as described in the section of this paper entitled Adjustment of Model Parameters.)

HEAT TRANSFER RATE BETWEEN SKIN AND AIR

The evaluation of the exchange coefficient characteristic of the heat transfer process between the skin and the ventilating air EX_{STA} was derived in a manner comparable to that described above for EX_{STL}, that is, through a consideration of experimental data corresponding to steady-state conditions.

The heat balance on the ventilating air during steady-state conditions is expressed as:

$$H_{ASENS} = H_{STA} + H_{SENSR} - H_{ATL} - H_L \quad (26a)$$

In more explicit terms, this equation can be expressed as:

$$H_{ASENS} = EX_{STA}(T_S - T_{AAVE}) + H_{SENSR} - EX_{ATL}(T_{AAVE} - T_{LAVE}) - H_L \quad (26b)$$

The quantities H_{ASENS}, T_S, T_{AAVE}, and T_{LAVE} are directly available from experimental data, and the evaluation of EX_{ATL} and H_L have previously been discussed. The remaining quantity, H_{SENSR}, can be calculated using the procedure described in the main body of this report. Consequently, a plot of $(H_{ASENS} - H_{SENSR} + H_{ATL} + H_L)$ versus $(T_S - T_{AAVE})$ for the steady-state experimental data will yield a slope value corresponding to EX_{STA}.

Such a plot is shown in figure 35. Unfortunately, the data points do not span a very wide range in the abscissa. Also, the ordinate values of the data are fairly widely dispersed. This dispersion can logically be attributed to the fact that the ordinate values are obtained from the algebraic sum of several experimental quantities, each of which have some associated error. Nonetheless, a value of EX_{STA} equal to 4.4 W/°C has been approximated from the average of the data shown in figure 35.

APPENDIX C

EVALUATION OF SYSTEM TIME CONSTANTS

The CSMP model of the LCG control loop which has been developed requires the mathematical description of the dynamic behavior of the elements comprising the control loop. The five elements considered to comprise the control loop are listed in table 4. Each element has been treated as a first order element, thus requiring a characteristic delay time and rise time for a mathematical description of its dynamic performance.

TABLE 4.– TIME CONSTANTS IN CONTROL LOOP

Element of control loop	Delay time, sec	Rise time, sec
Air ventilation garment (inlet to outlet)	1.7	28.0
Air umbilical to hygrometer output	4.4	16.0
Controller input to valve output	1.1	3.8
Valve output to LCG inlet	11.0	15.0
Liquid cooled garment (inlet to outlet)	7.4 (1.5[a])	21.0 (5.0[a])

[a]Modified for CSMP use

The values of the delay times and rise times given in table 4 were determined by five separate experiments. Each experiment involved isolating the element while still maintaining the normal functioning of the element (i.e., flow of air or water), imposing a step change at the inlet to the element, and recording the dynamic response at the exit from the element.

The results of these experiments in general justified the assumption of treating the elements as first order. Any departures were considered slight enough to ignore. The values given in table 4, with the exception of those listed for the LCG, are the average experimental values subsequently used in the CSMP program. For the case of the LCG, the values enclosed in parentheses were actually used in the CSMP program, while the other two values are the experimentally determined ones. The reduced times used in the CSMP program were selected so as to dampen the fluctuations initially noted in the CSMP results for H_{LCG} occurring whenever the computed T_{LI} underwent a rapid change. Reducing these two characteristic times allowed the computed H_{LCG} to behave more nearly as the experimental counterpart, and this fact was considered adequate justification to make the change. Physical support for the change is that the heat balance on the LCG employed in the CSMP model does not ascribe any thermal capacity to the LCG, but rather approximates this dynamic feature by the use of delay and rise times.

REFERENCES

1. Nunneley, Sarah A.: Water Cooled Garments: A Review. Space Life Sci., vol. 2, 1970, pp. 335–360.

2. Webb, Paul; Annis, J. F.; and Troutman, S. J.: Automatic Control of Water Cooling in Space Suits. NASA CR–1085, 1968.

3. Webb, Paul; Troutman, Samuel J.; and Annis, J. F.: Automatic Cooling in Water Cooled Space Suits. Aerospace Med., vol. 41, no. 3, March 1970, pp. 260–277.

4. Merrill, G. L.; and Starr, J. B.: Automatic Temperature Control for Liquid-Cooled Flight Suits. U.S. Naval Air Development Center, NADC–AC–6702, 1967.

5. Starr, J. B.: Fluidic Temperature Control System for Liquid-Cooled Space Suits, NASA Conference on Portable Life Support Systems, April 30 – May 2, 1969. NASA SP–234, 1970, pp. 179–189. (See also NASA CR–108330, 1970.)

6. Troutman, S. J., Jr.; and Webb, Paul: Automatic Control of Water Cooled Suits From Differential Temperature Measurements. NASA CR–86244, 1969.

7. Troutman, S. J., Jr.; and Webb, Paul: Automatic Controllers for the Apollo LCG. NASA CR–108540, 1970.

8. Fulcher, Clay W. G.: Control of a Liquid Cooling Garment for Extravehicular Astronauts by Cutaneous and External Auditory Meatus Temperatures. NASA CR–115122, 1971.

9. Chambers, Alan B.: Controlling Thermal Comfort in the EVA Space Suit. ASHRAE J., March 1970, pp. 33–38.

10. Gagge, A. P.; Stolwijk, J. A. J.; and Hardy, J. D.: Comfort and Thermal Sensations and Associated Physiological Responses at Various Ambient Temperatures. Environmental Res., vol. 1, 1967, pp. 1–20.

11. DuBois, D.; and DuBois, E. F.: A Formula to Estimate the Approximate Surface Area if Height and Weight be Known. Arch. Internal Med. vol. 17, 1916, pp. 863–871.

12. Sloan, A. W.; and Weir, J. B.: Nomograms for Prediction of Body Density and Total Body Fat From Skin Fold Measurements. J. Appl. Phys., vol. 28, no. 2, Feb. 1970, pp. 221–222.

13. Camacho, A.; Robertson, W.; and Walther, A.: Study of Man Pulling a Cart on the Moon. NASA CR–1697, 1971.

14. Passmore, R.; and Durnin, J.V.G.A.: Human Energy Expenditure. Phys. Rev., vol. 35, 1955, pp. 801–840.

15. Hardy, J. D.; and DuBois, E. F.: The Technique of Measuring Radiation and Convection. J. Nutr., vol. 15, 1938, pp. 461–475.

16. Anon.: System/360 Continuous System Modeling Program User's Manual. IBM Rep. H20–0367–3.

17. Winton, Henry J.: Computer Model of Human Thermoregulation. Ph.D. Dissertation to Department of Electrical Engineering, Univ. of Santa Clara, Santa Clara, California, 1971.

18. Winton, Henry J.; and Linebarger, Robert N.: Computer Simulation of Human Temperature Control. Simulation, vol. 15, no. 5, Nov. 1970, pp. 213–221.

19. Benzinger, T. H.: Heat Regulation: Homeostasis of Central Temperature in Man. Physiological Reviews, vol. 49, no. 4, October 1969, pp. 671–759.

20. Rushmer, Robert F.: Cardiovascular Dynamics. W. B. Sanders & Co., Philadelphia, 1970.

21. Greenfield, A. D. M.: The Circulation Through the Skin. Handbook of Physiology. Section 2, Circulation, vol. II, Chapter 39, American Physiological Society, Washington, D. C., 1963, pp. 1325–1351.

22. Barcroft, Henry: Circulation in Skeletal Muscle. Handbook of Physiology. Section 2, Circulation, vol. II, Chapter 40, American Physiological Society, Washington, D. C., 1963, pp. 1353–1385.

23. Hammel, Harold T.: Concept of the Adjustable Set Temperature, Chapter 46 in Physiological and Behavioral Temperature Regulation, Charles C. Thomas Publisher, Springfield, Illinois, 1970, pp. 676–683.

24. Astrand, Per-Olof; and Rodahl, Kaare: Textbook of Work Physiology, McGraw-Hill Book Co., New York, 1970, p. 208.

25. Stolwijk, J. A. J.; Saltin, B.; and Gagge, A. P.: Physiological Factors Associated with Sweating During Exercise. Aerospace Med., vol. 39, no. 10, Oct. 1968, pp. 1101–1105.

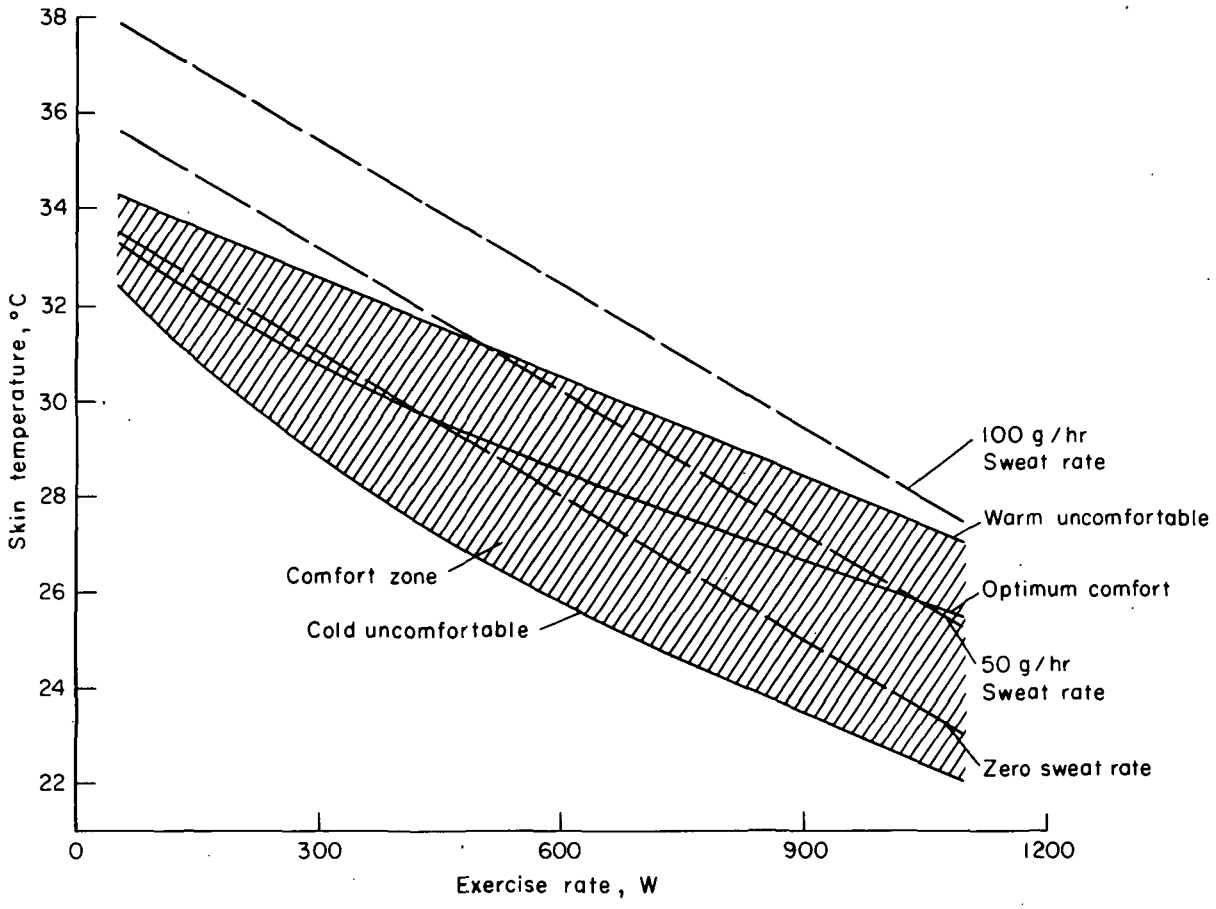

Figure 1.– Subjective comfort zone in relation to skin temperature, sweat rate, and exercise rate.

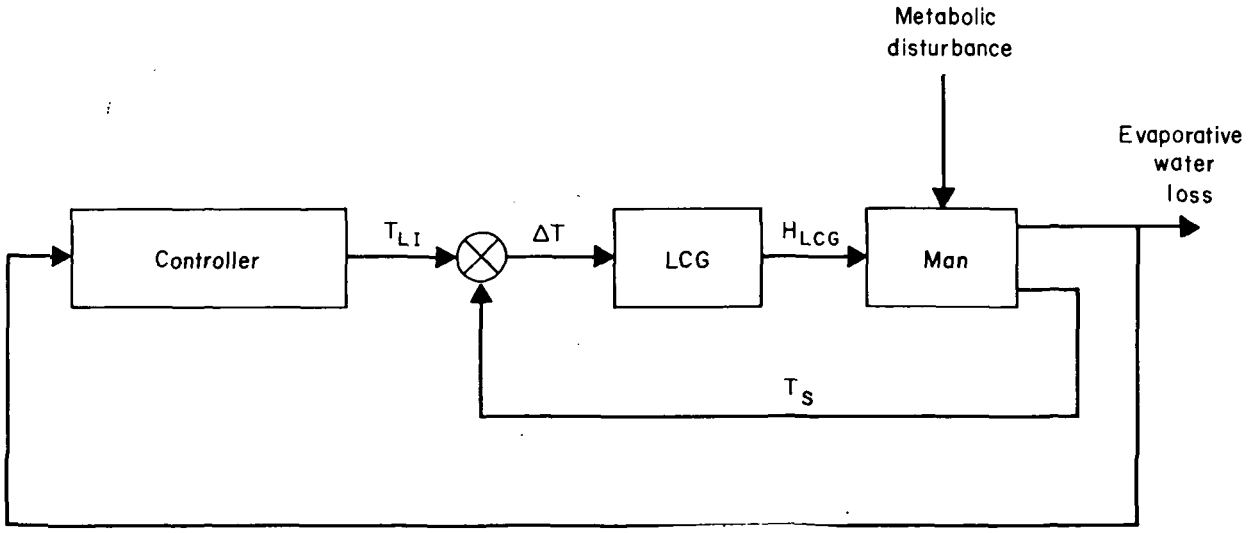

Figure 2.– Schematic illustration of the interactions among man, his LCG, and the LCG temperature controller based on evaporative water loss rate.

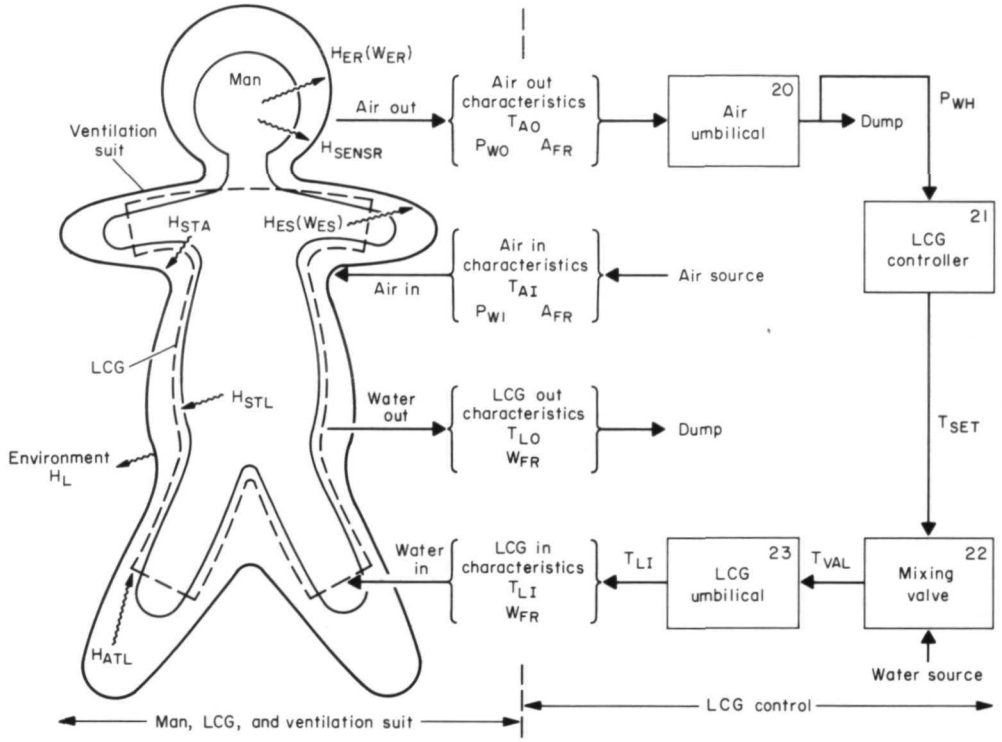

Figure 3.– Schematic model illustrating the heat balance parameters considered in the study.

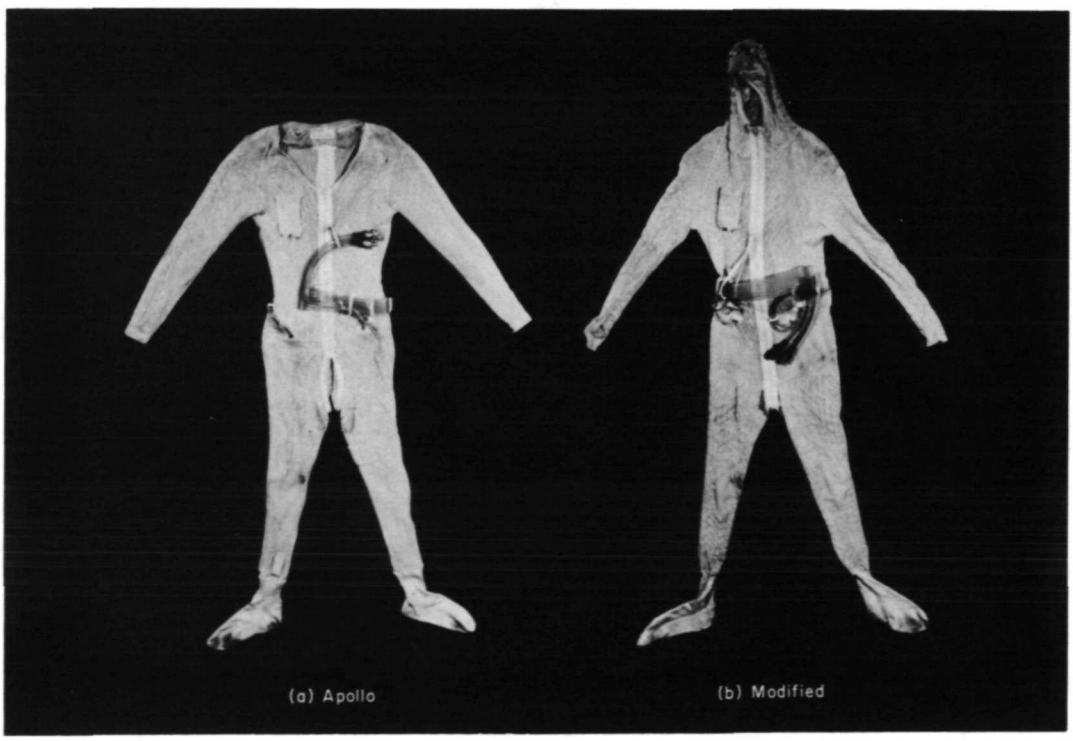

Figure 4.– Liquid-cooling garments used in the tests.

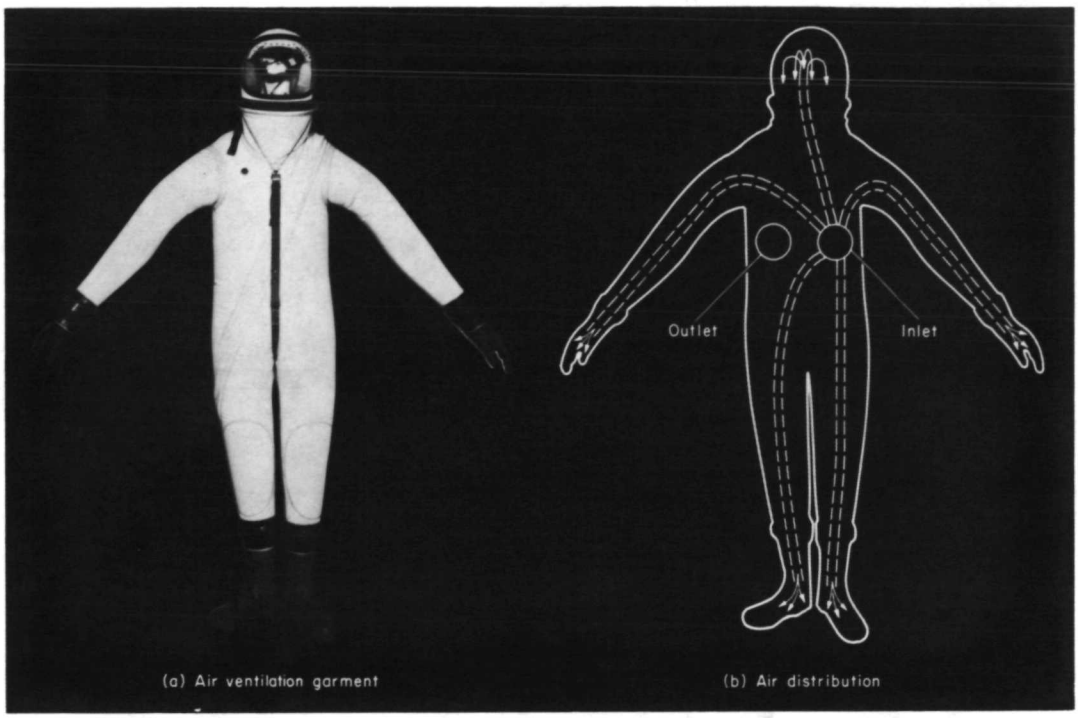

Fibure 5.– Air ventilation garment used in the tests.

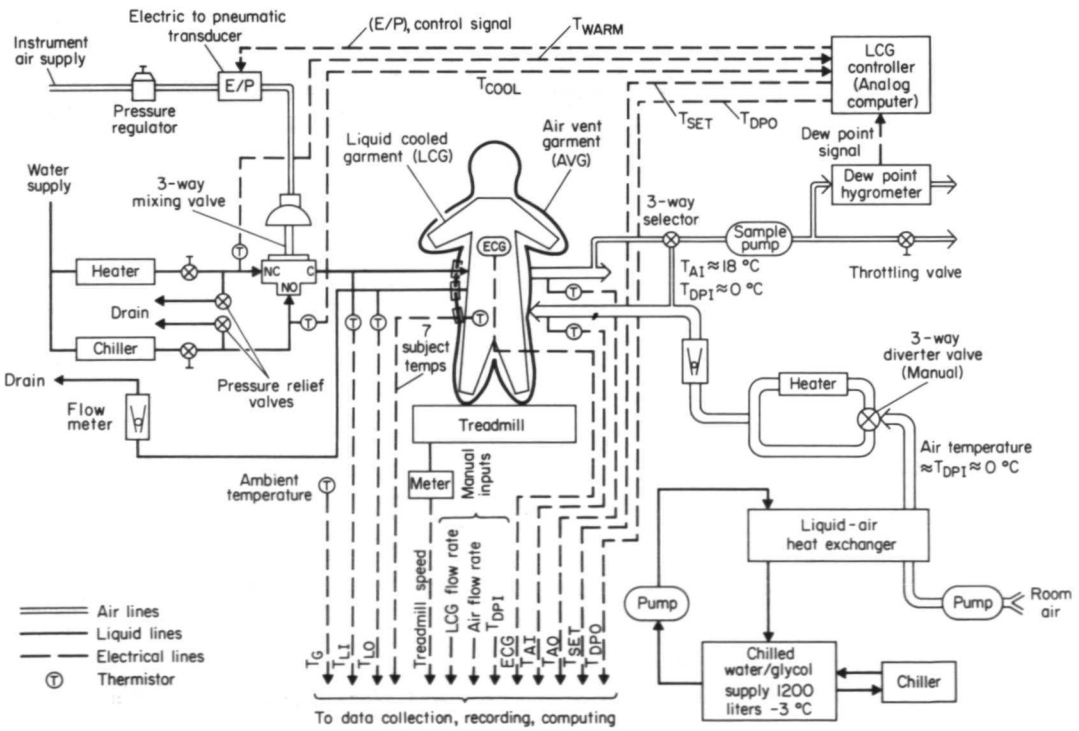

Figure 6.– Test apparatus and instrumentation.

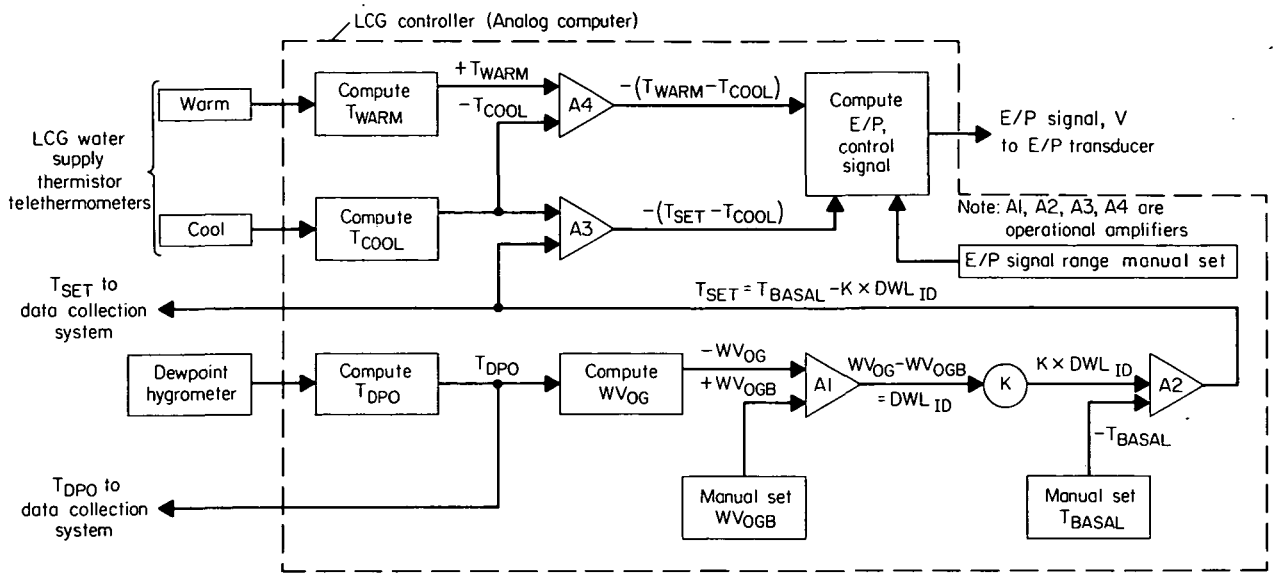

Figure 7.– Schematic diagram of the LCG temperature controller.

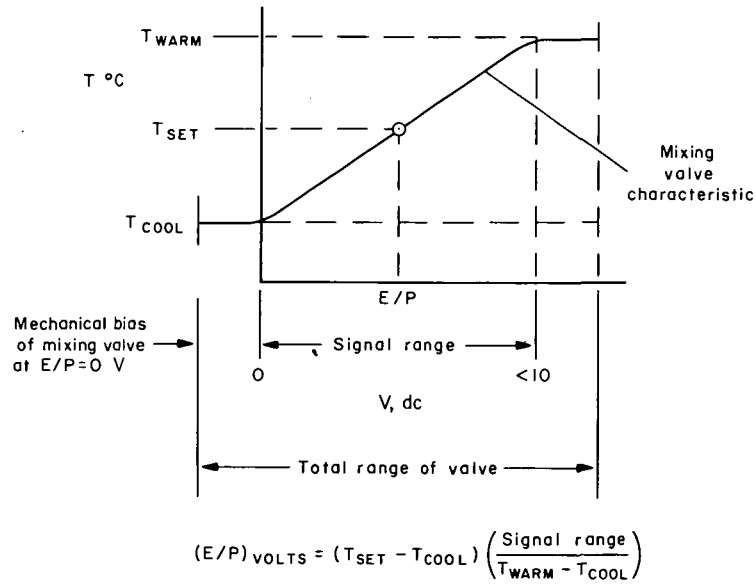

Figure 8.– Mixing valve operating and control characteristics.

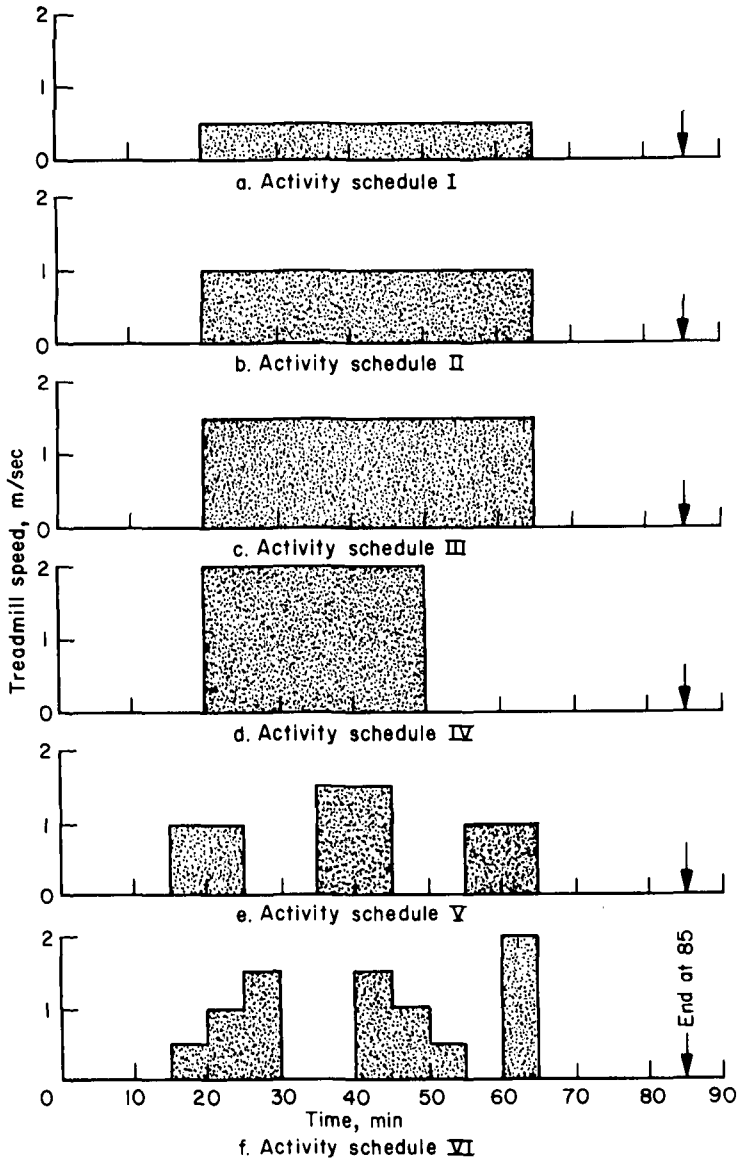

Figure 9.– Activity schedules for the tests.

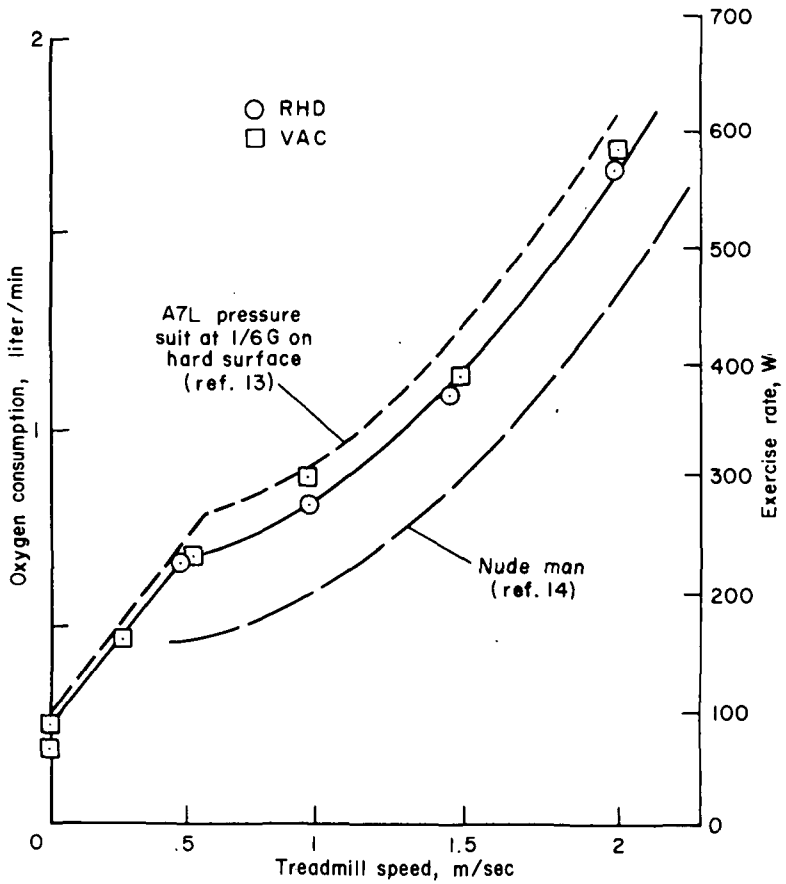

Figure 10.– Oxygen consumption and exercise rate as a function of treadmill speed.

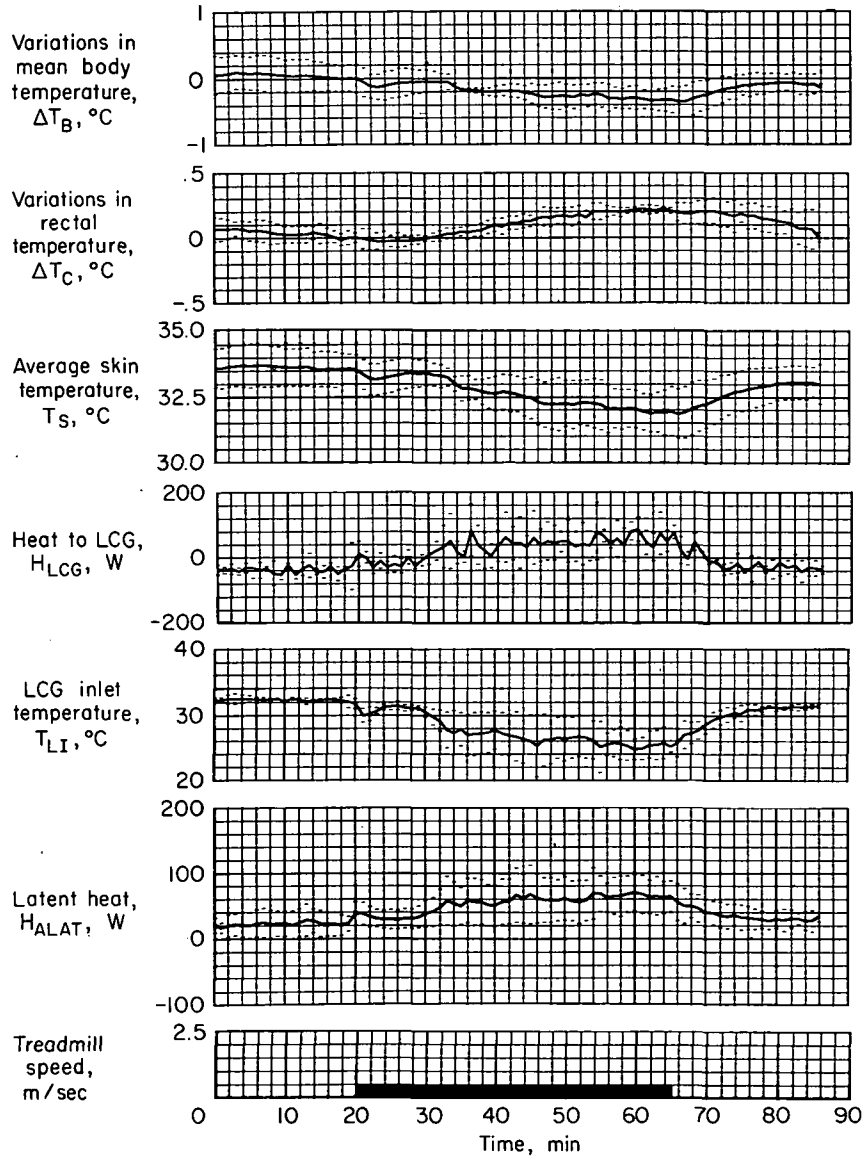

Figure 11.– Averaged experimental results for the three subjects wearing the Apollo-type LCG; activity schedule I, test 1 (treadmill speed: 1/2 m/sec).

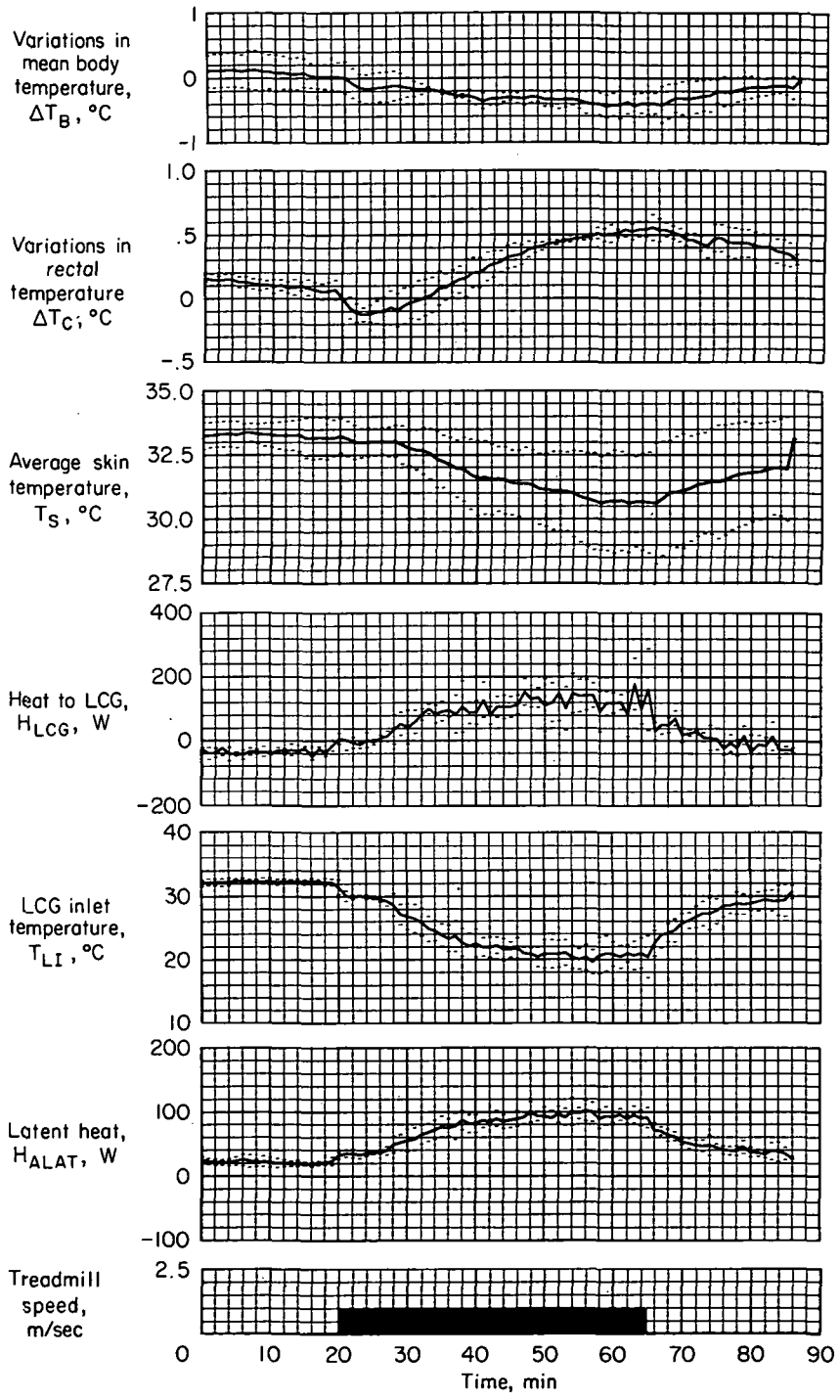

Figure 12.– Averaged experimental results for the three subjects wearing the Apollo-type LCG; activity schedule II, test 2 (treadmill speed: 1 m/sec).

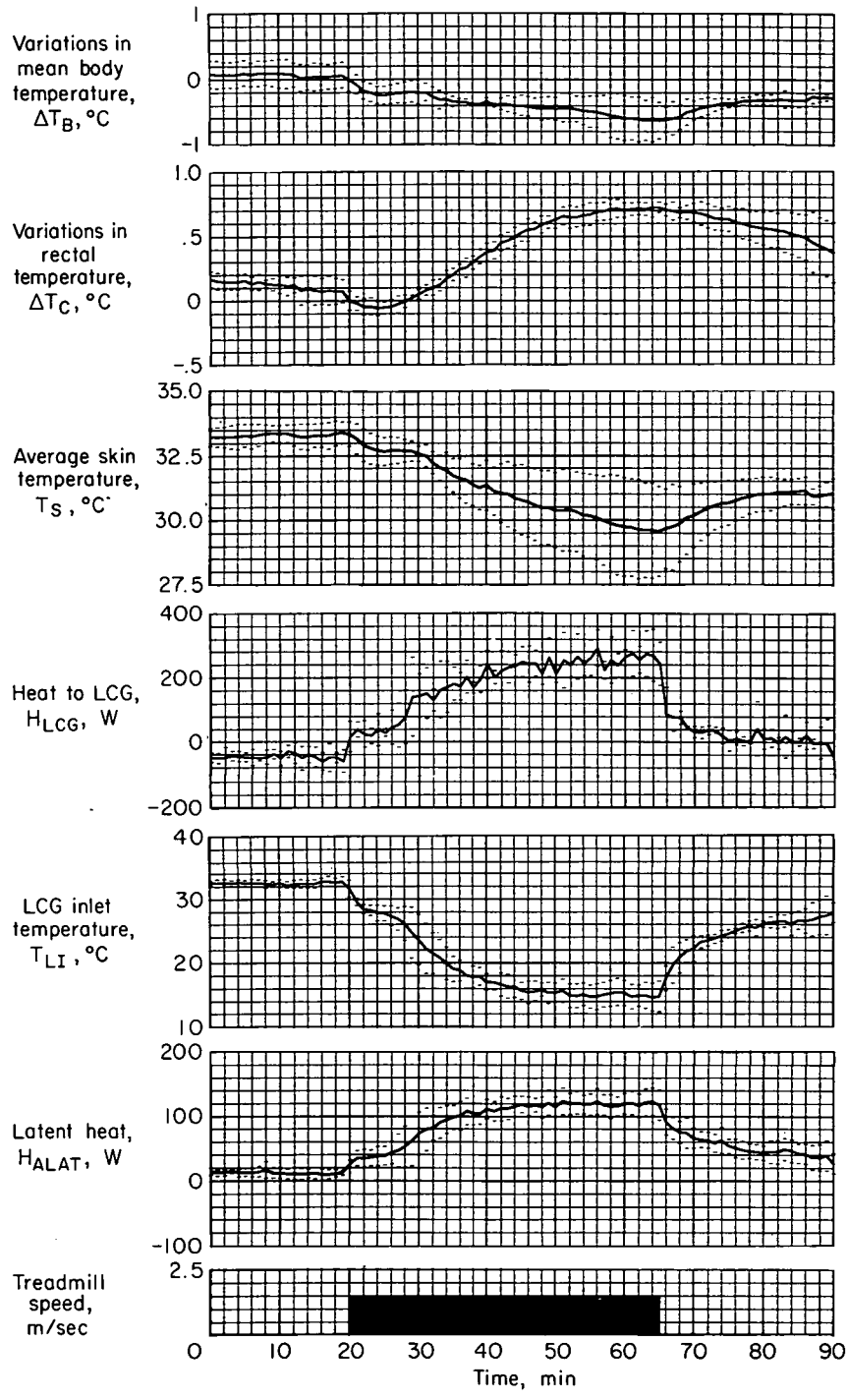

Figure 13.– Averaged experimental results for the three subjects wearing the Apollo-type LCG; activity schedule III, test 3 (treadmill speed: 1-1/2 m/sec).

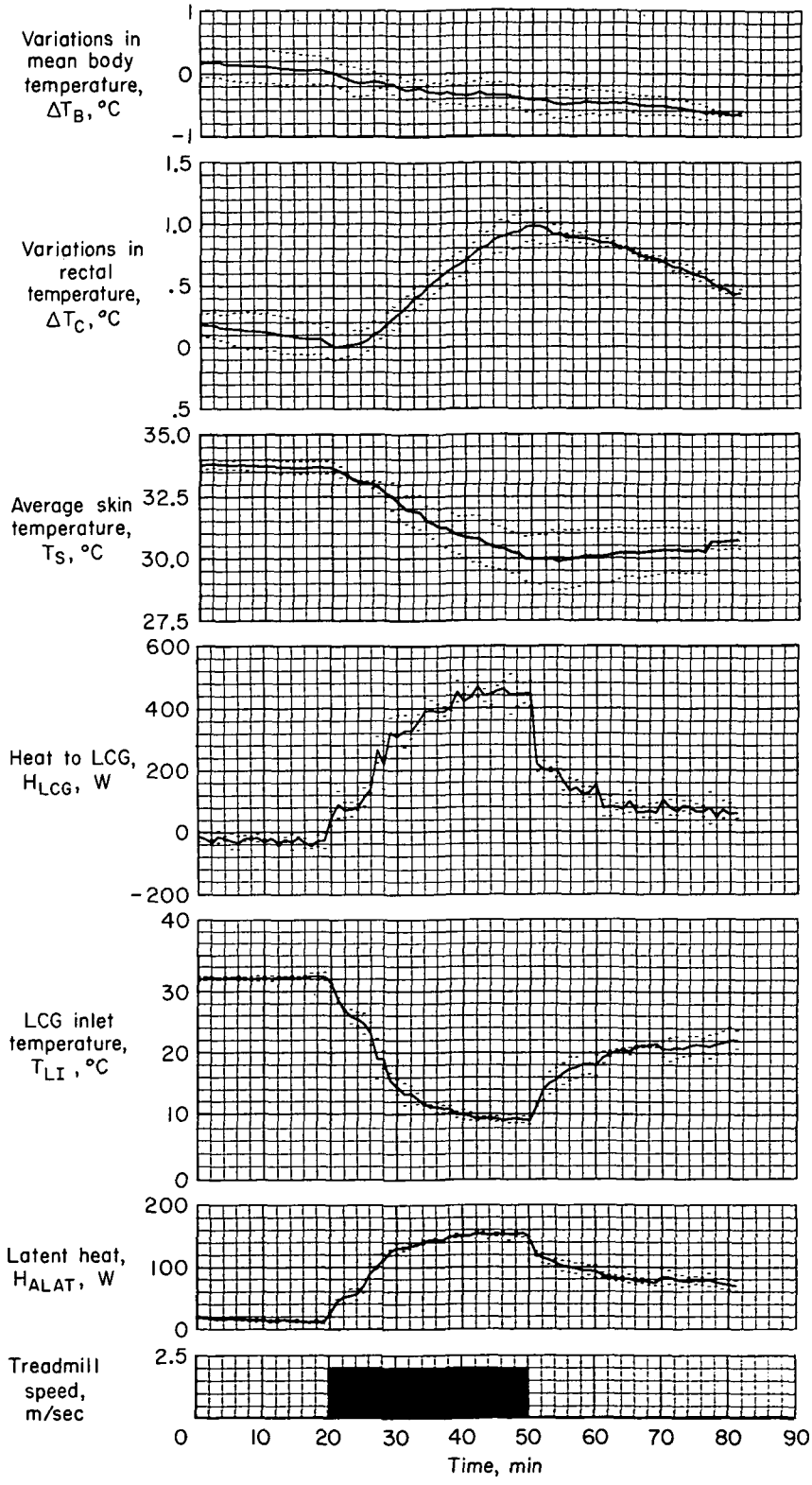

Figure 14.– Averaged experimental results for the three subjects wearing the Apollo-type LCG; activity schedule IV, test 4 (treadmill speed: 2 m/sec).

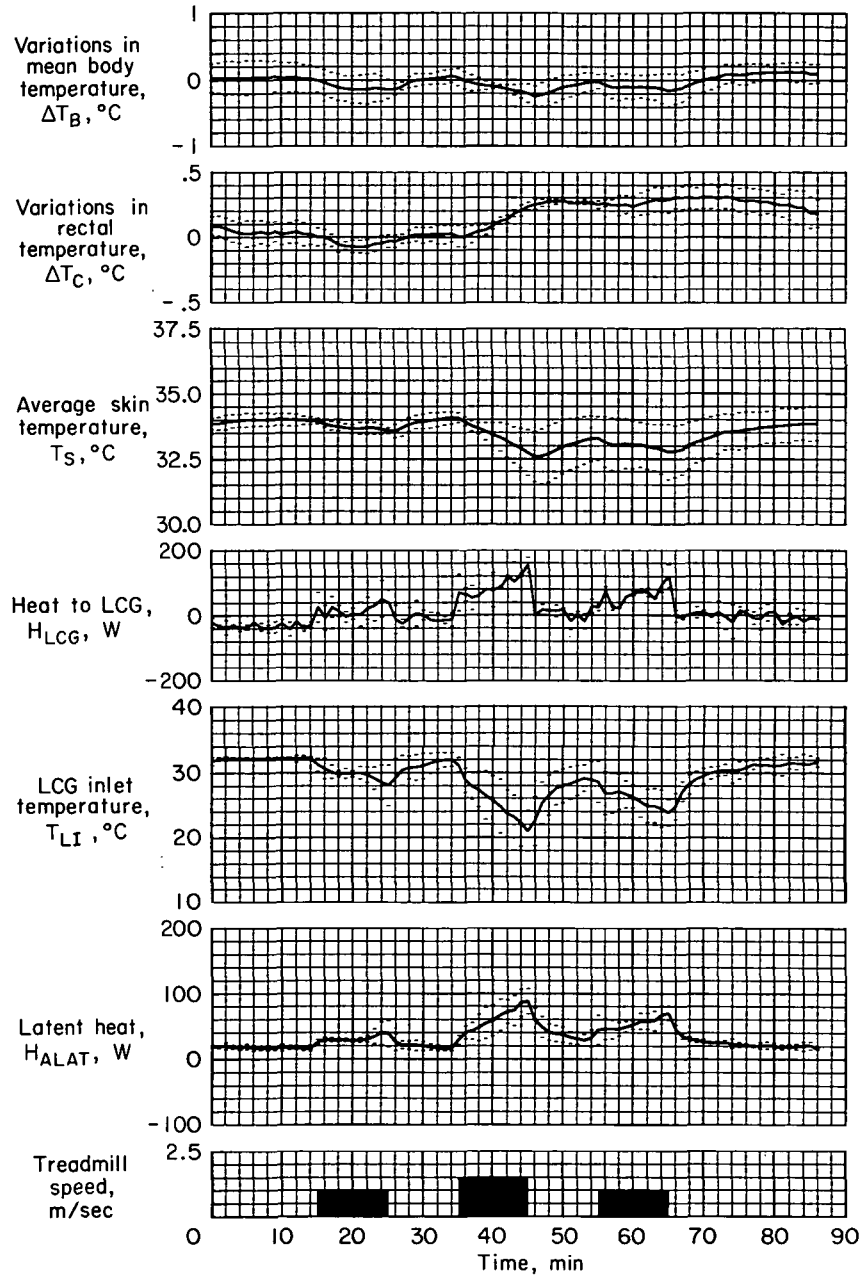

Figure 15.– Averaged experimental results for the three subjects wearing the Apollo-type LCG; activity schedule V, test 5 (treadmill speeds: 1, 1-1/2, 1 m/sec).

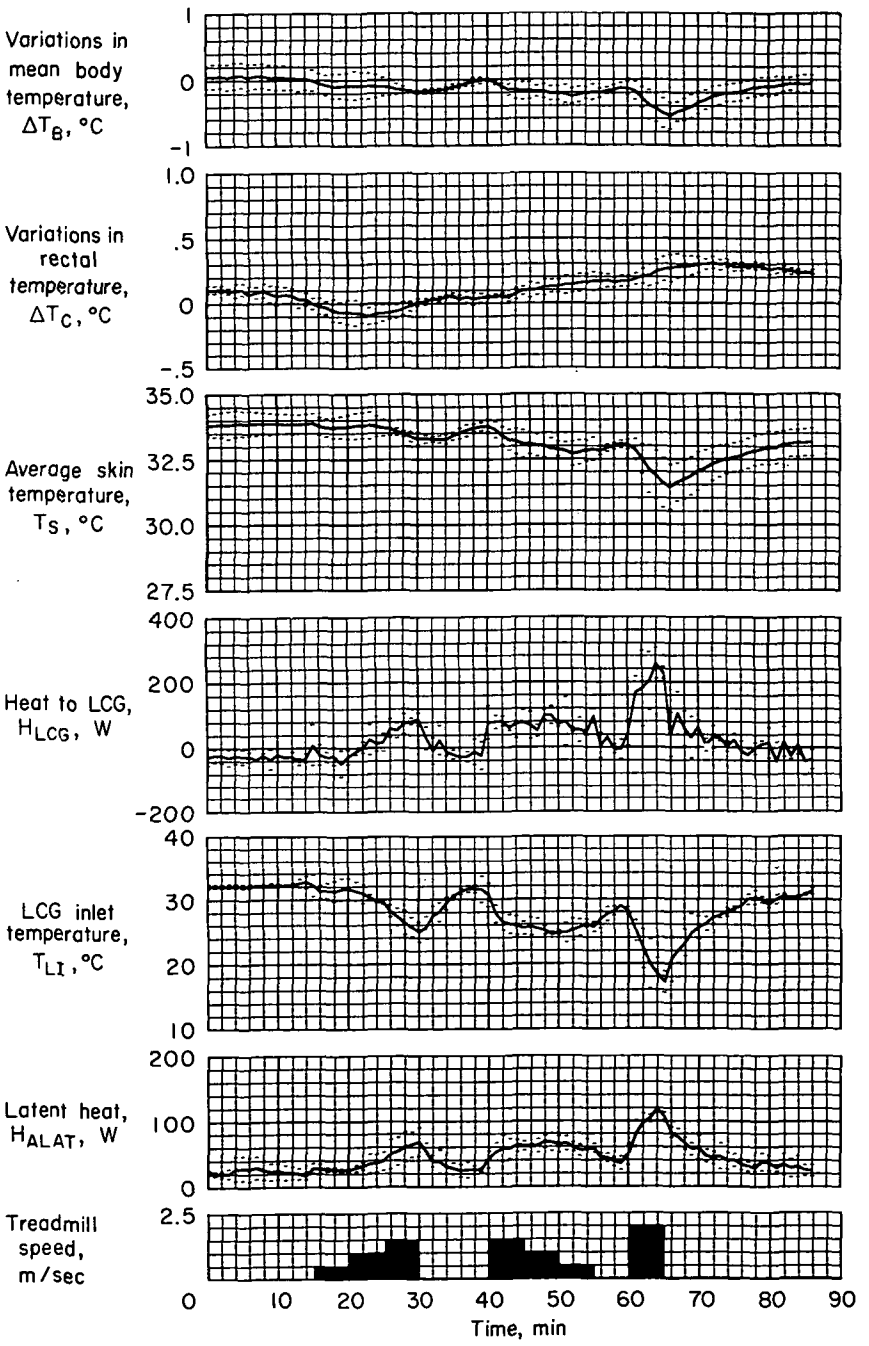

Figure 16.– Averaged experimental results for the three subjects wearing the Apollo-type LCG; activity schedule VI, test 6 (treadmill speeds: 1/2 – 1-1/2, 1-1/2 – 1/2, 2 m/sec).

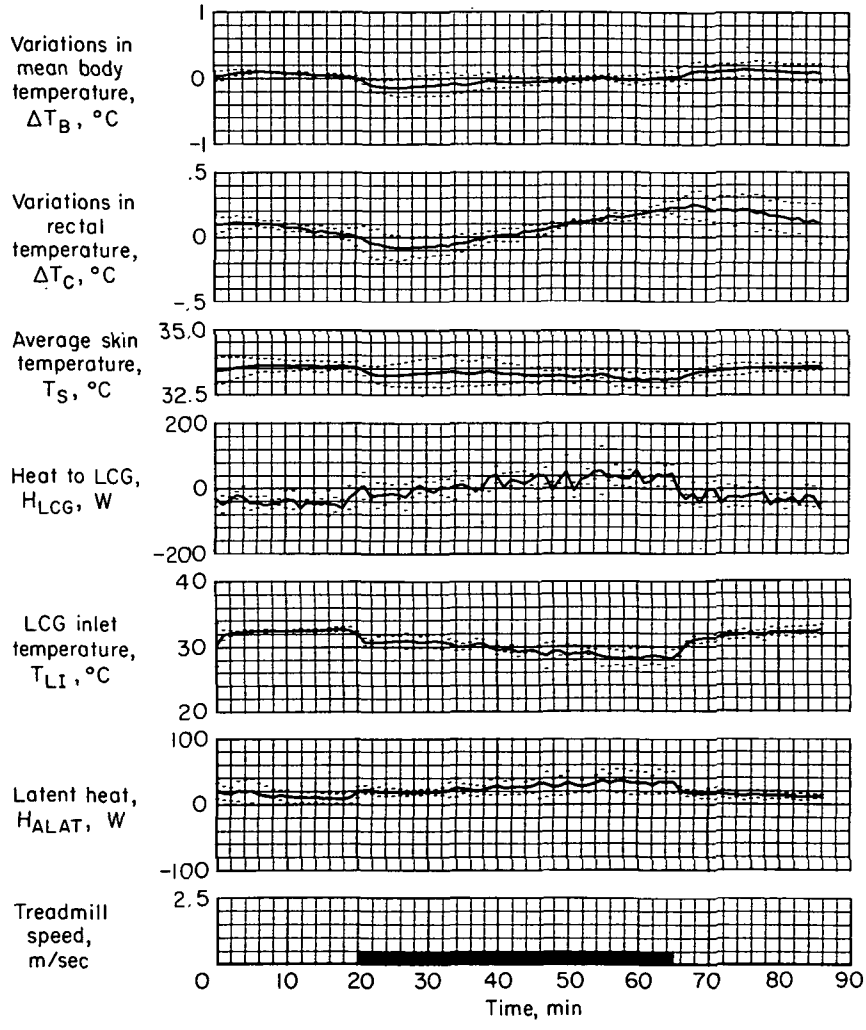

Figure 17.– Averaged experimental results for the three subjects wearing the modified LCG, activity schedule I, test 7 (treadmill speed: 1/2 m/sec).

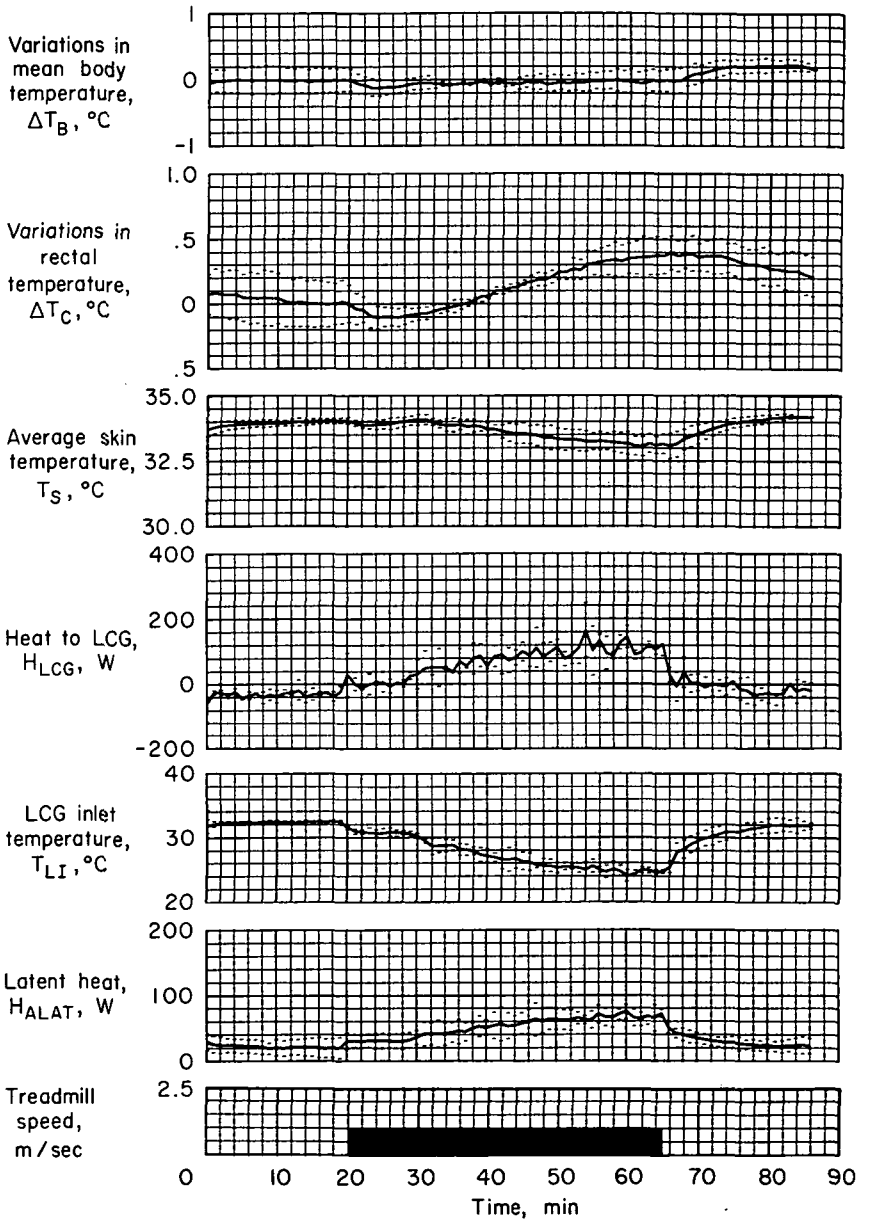

Figure 18.– Averaged experimental results for the three subjects wearing the modified LCG; activity schedule II, test 8 (treadmill speed: 1 m/sec).

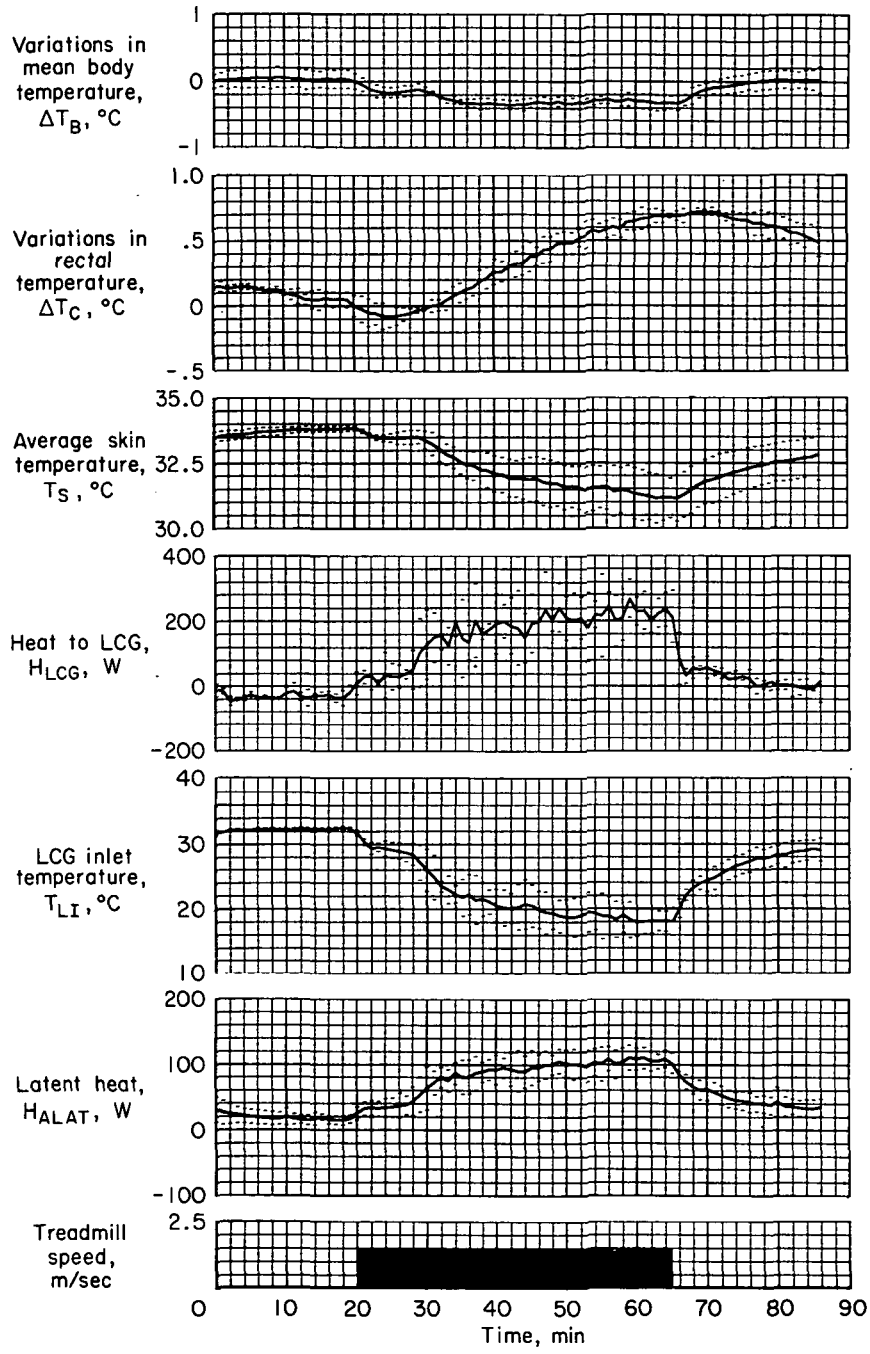

Figure 19.– Averaged experimental results for the three subjects wearing the modified LCG; activity schedule III, test 9 (treadmill speed: 1-1/2 m/sec).

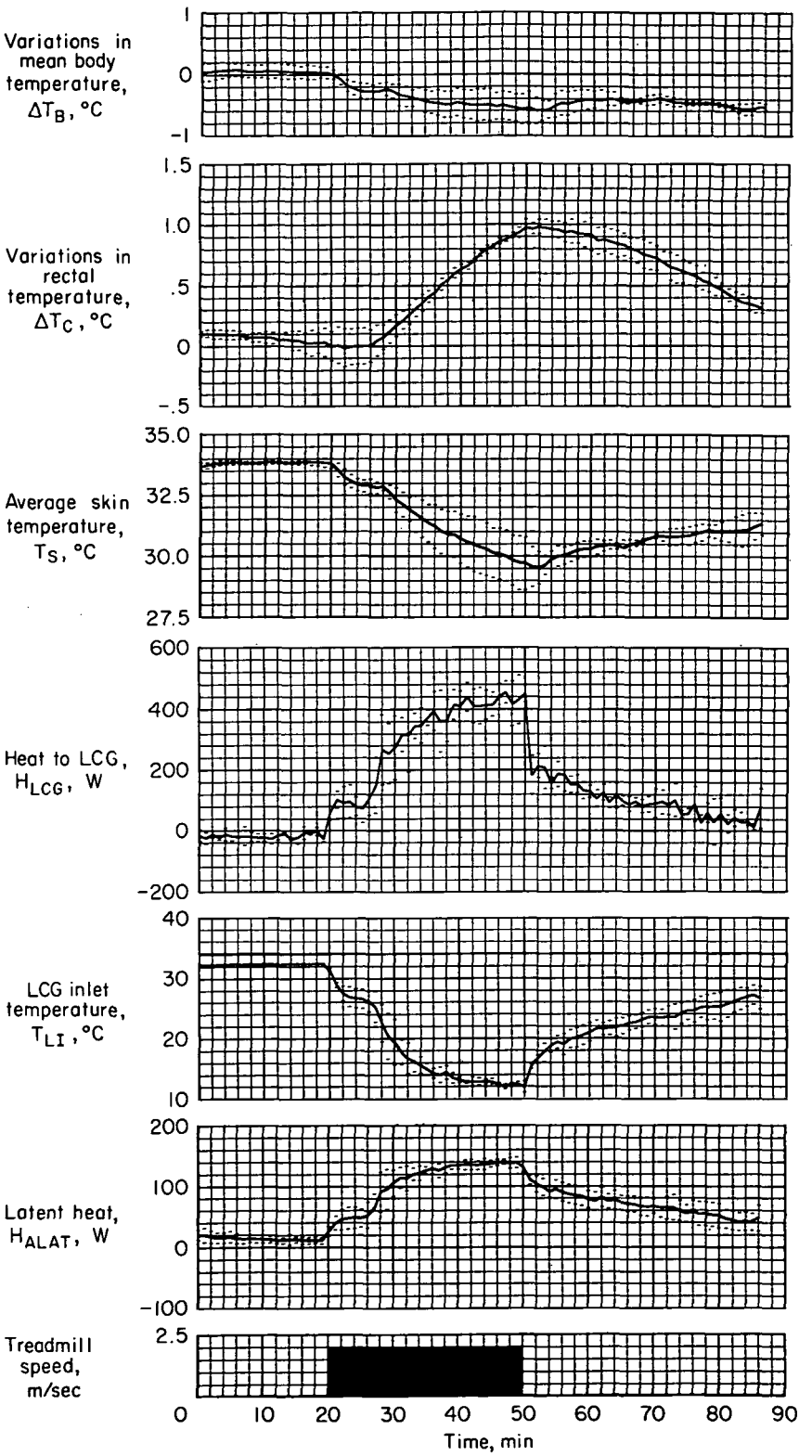

Figure 20.– Averaged experimental results for the three subjects wearing the modified LCG, activity schedule IV, test 10 (treadmill speed: 2 m/sec).

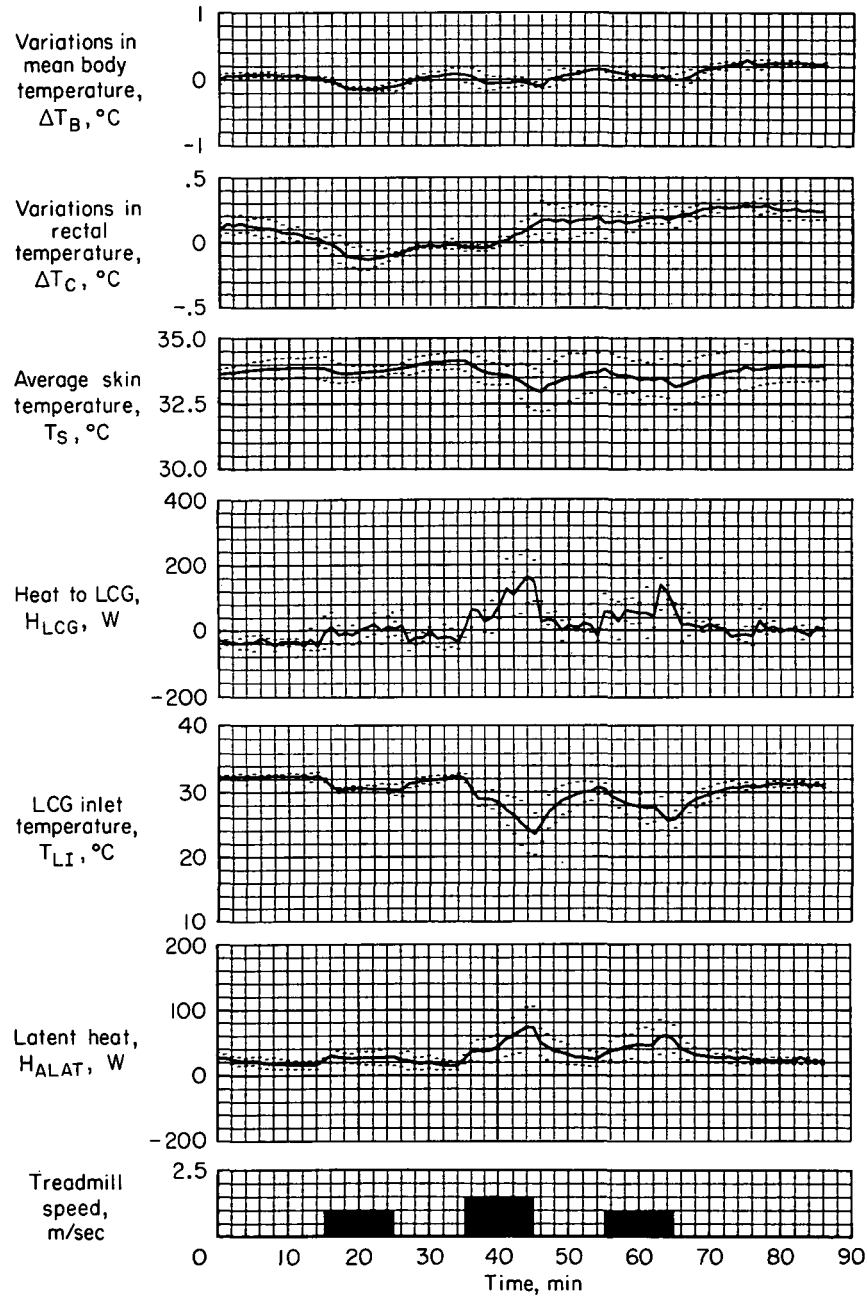

Figure 21.– Averaged experimental results for the three subjects wearing the modified LCG; activity schedule V, test 11 (treadmill speeds: 1, 1-1/2, 1 m/sec).

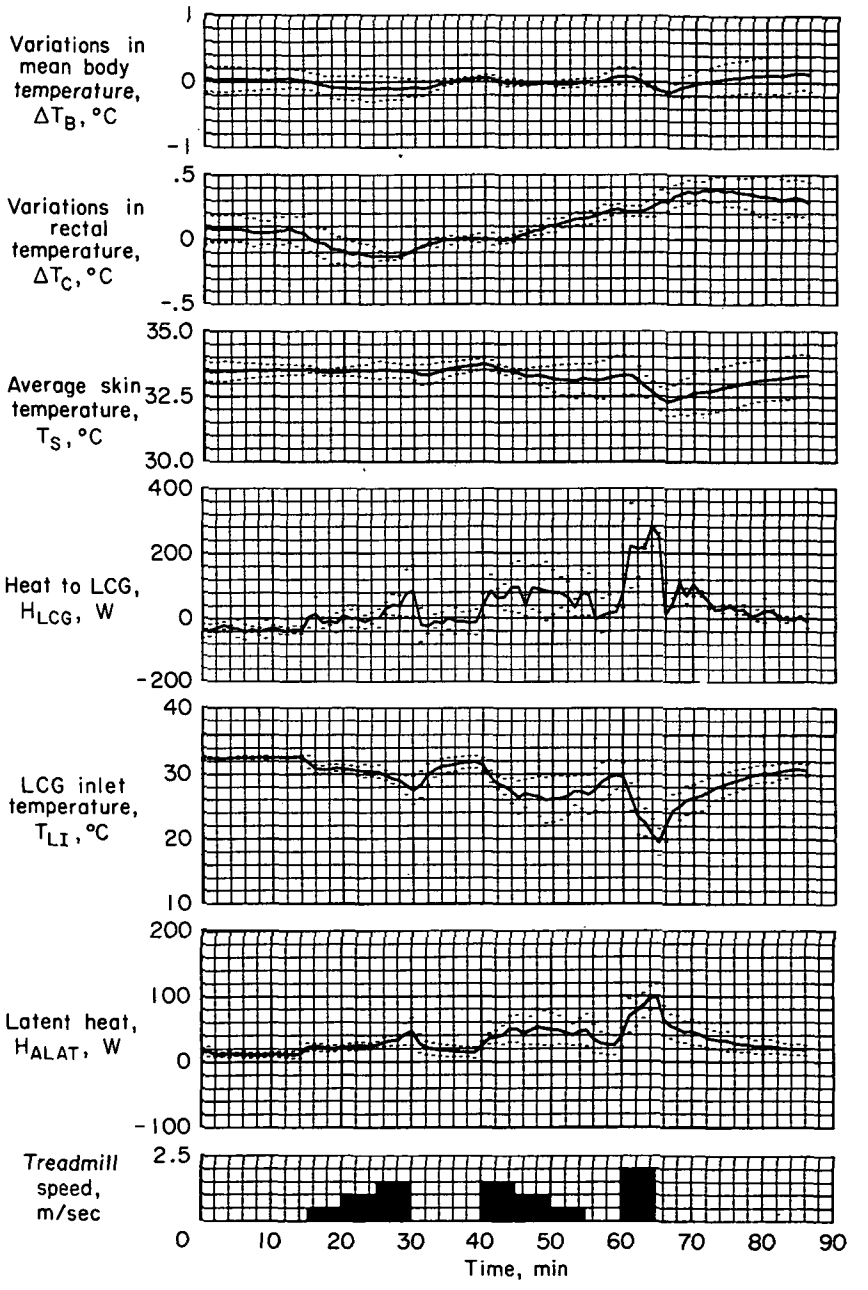

Figure 22.– Averaged experimental results for the three subjects wearing the modified LCG; activity schedule VI, test 12 (treadmill speeds: 1/2 – 1-1/2, 1-1/2 – 1/2, 2 m/sec).

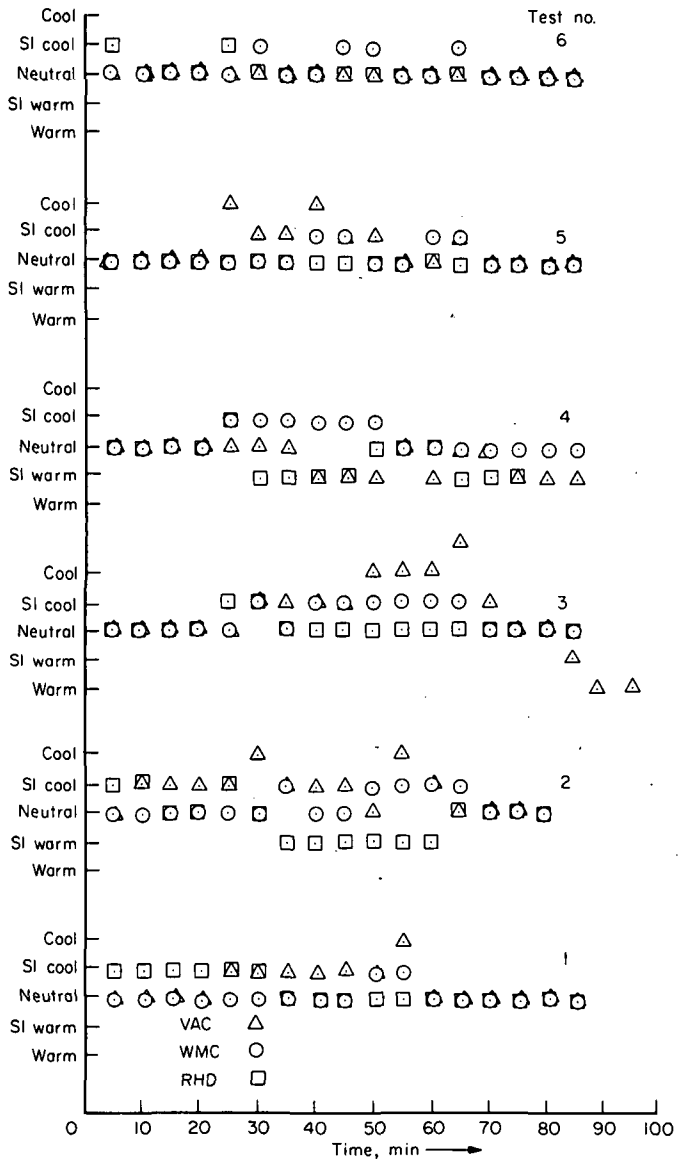

Figure 23.– Subjective comments on thermal sensation for subjects wearing the Apollo-type LCG.

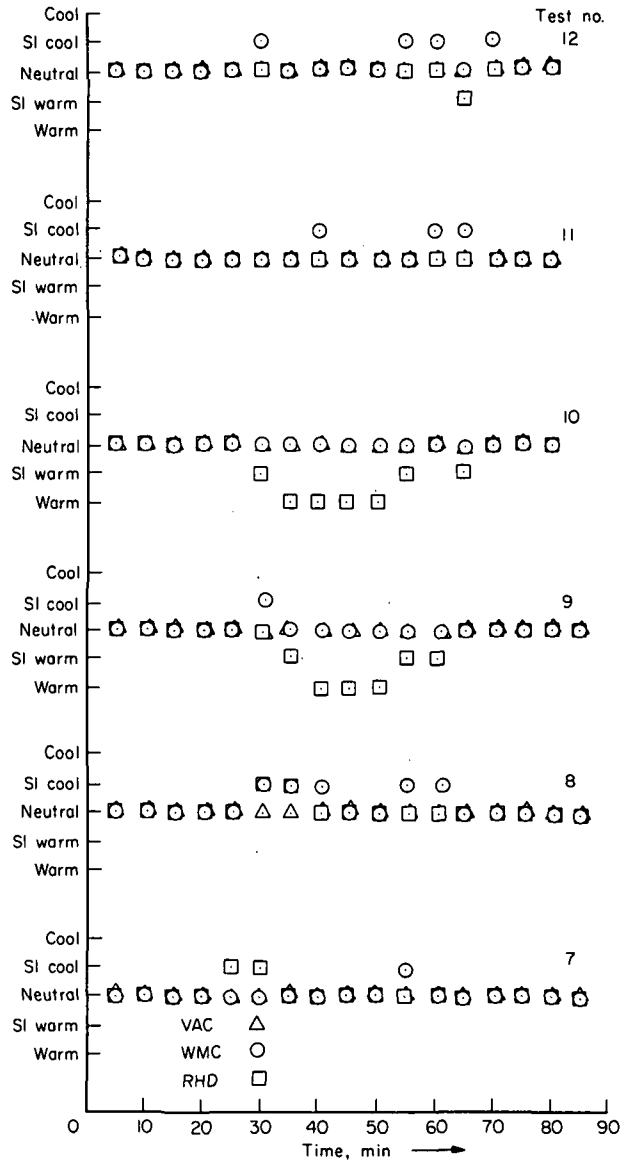

Figure 24.– Subjective comments on thermal sensation for subjects wearing the modified LCG.

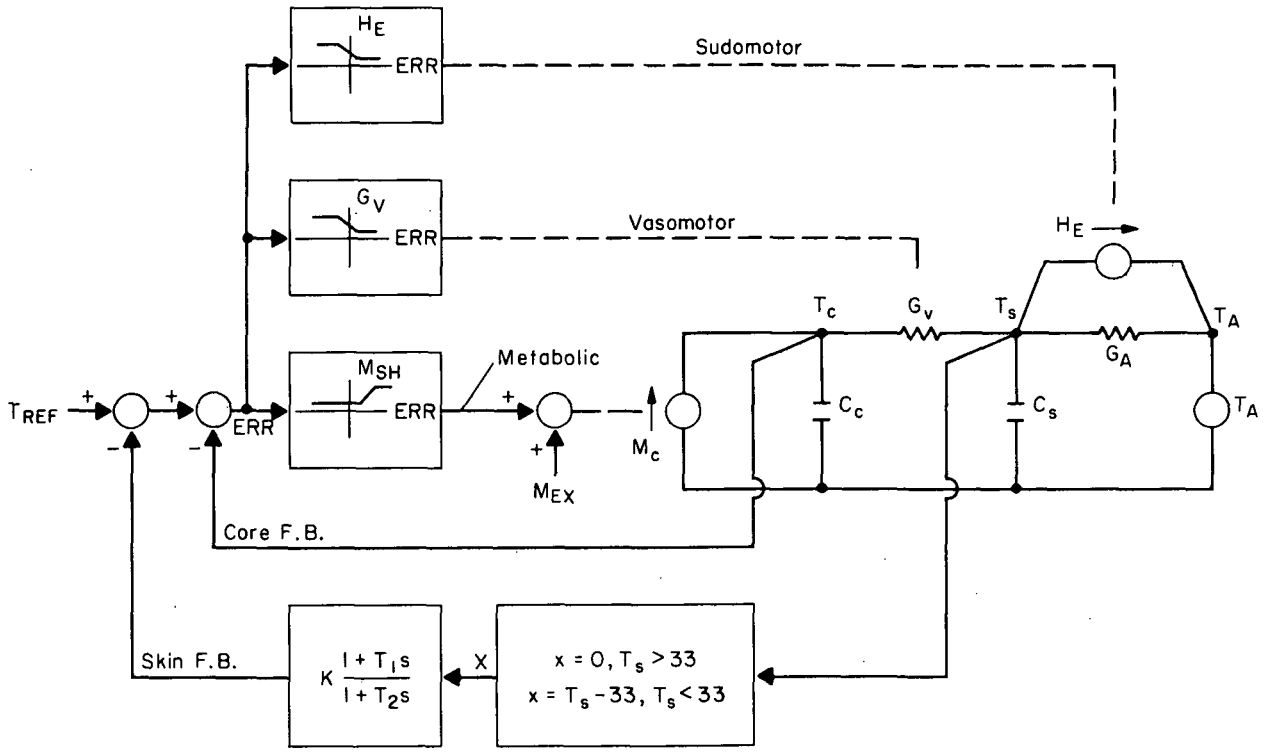

Figure 25.– Winton's feedback model of human thermoregulation (two-layer).

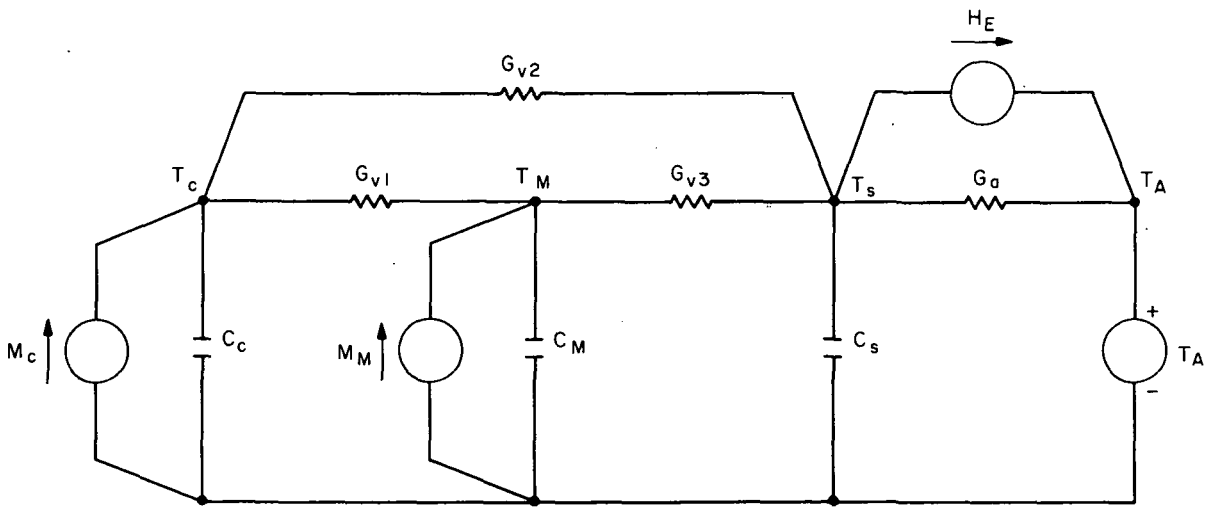

Figure 26.– Winton's feedback model of human thermoregulation (three-layer).

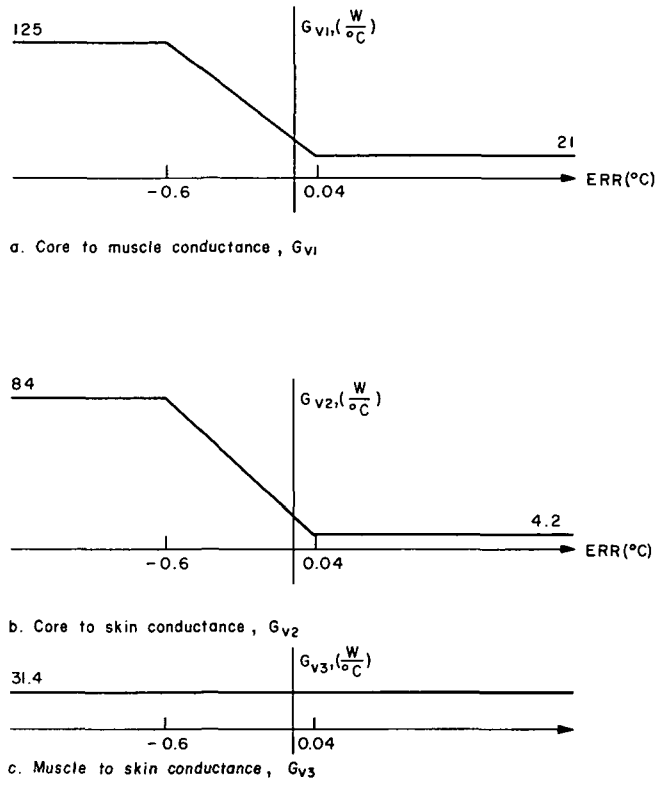

Figure 27.– Winton's three-layer vasomotor control functions.

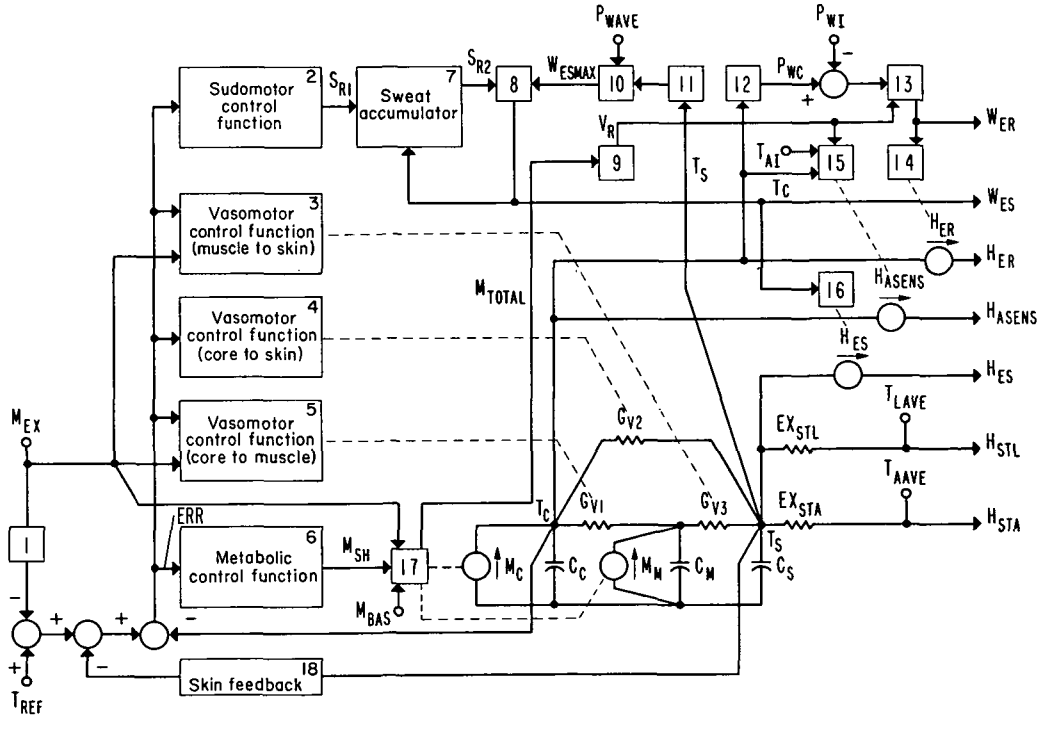

Figure 28.– Revised feedback model of human thermoregulation.

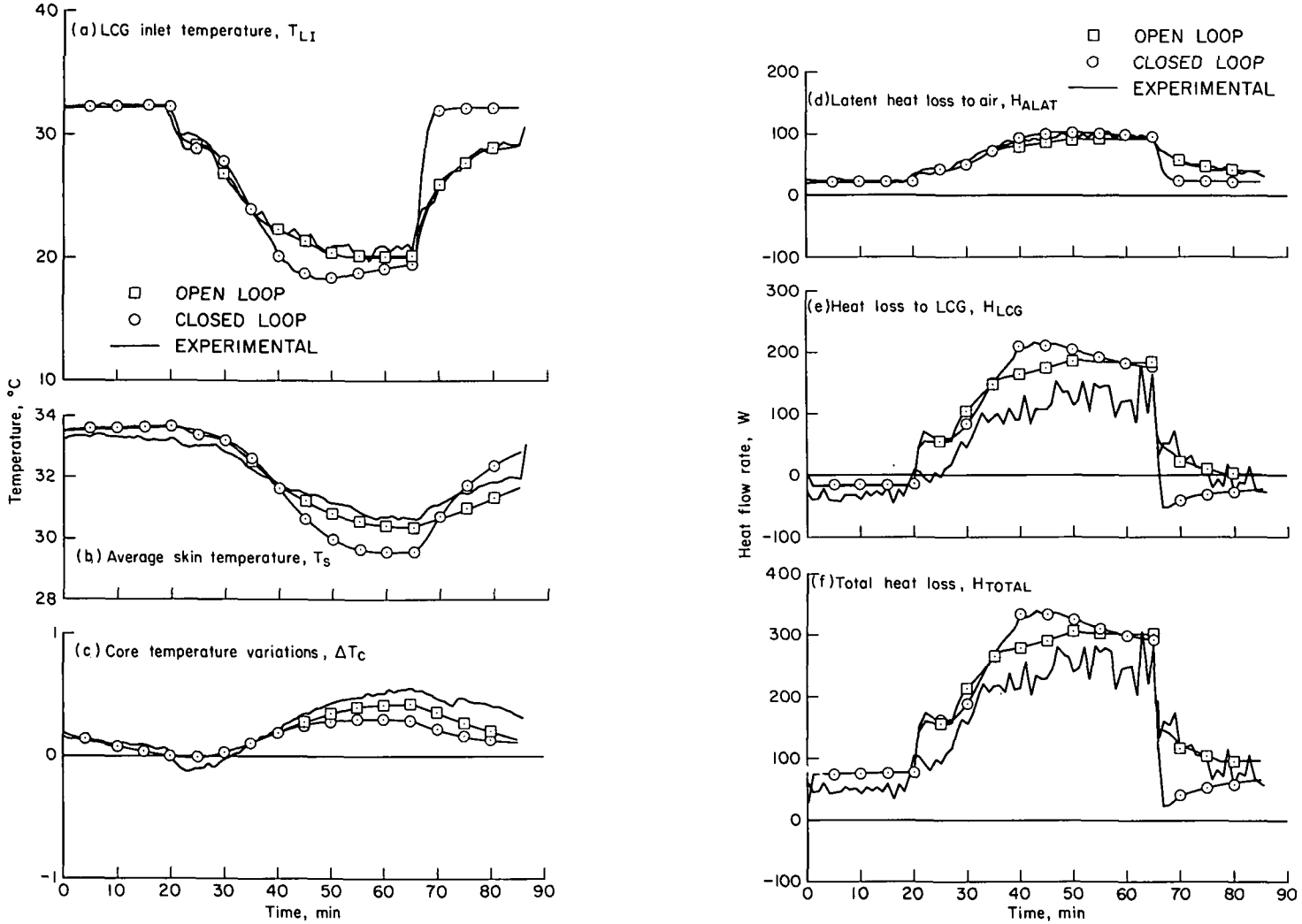

Figure 29.— CSMP simulations; activity schedule II (treadmill speed, 1 m/sec).

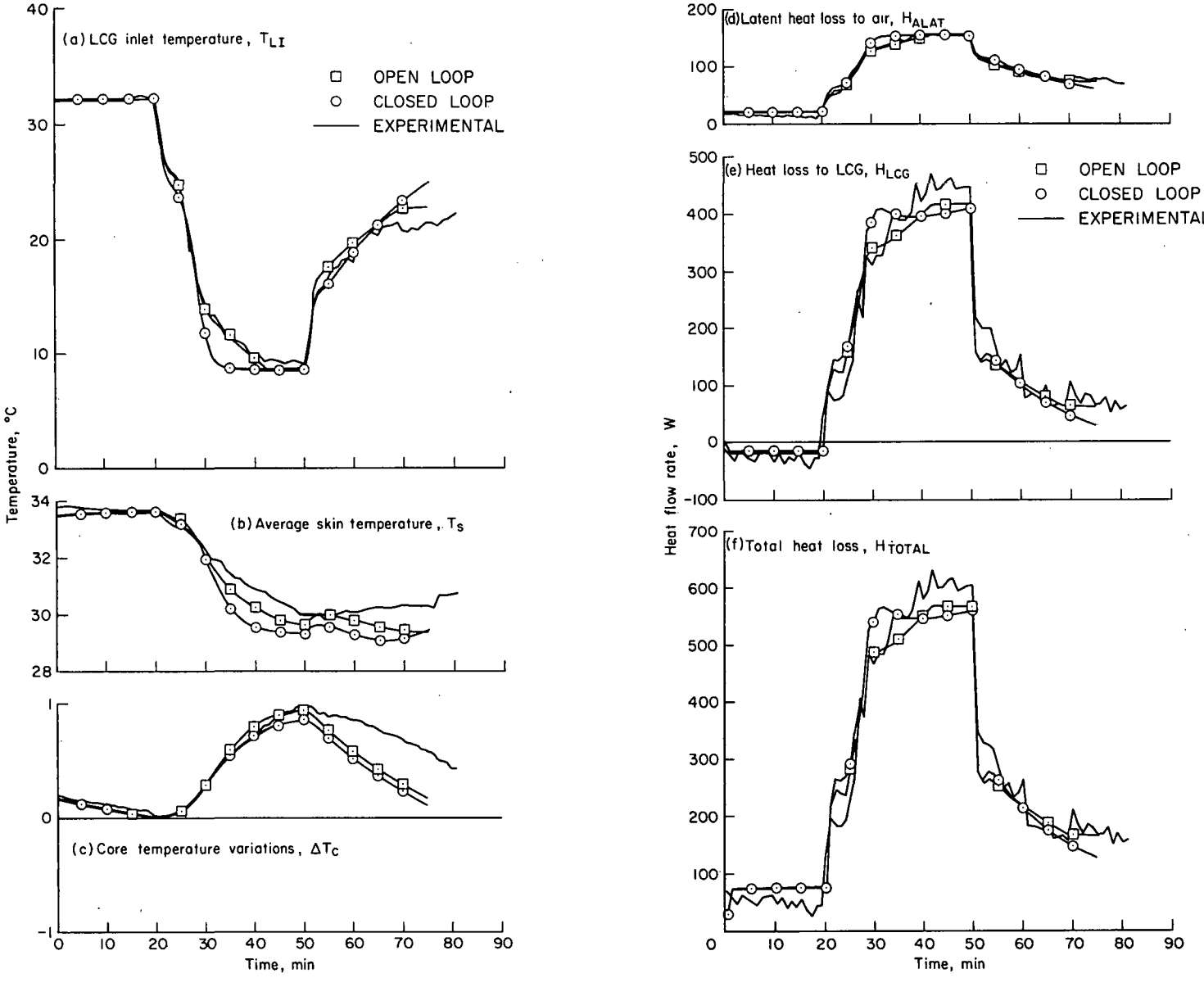

Figure 30.– CSMP simulations; activity schedule IV (treadmill speed, 2 m/sec).

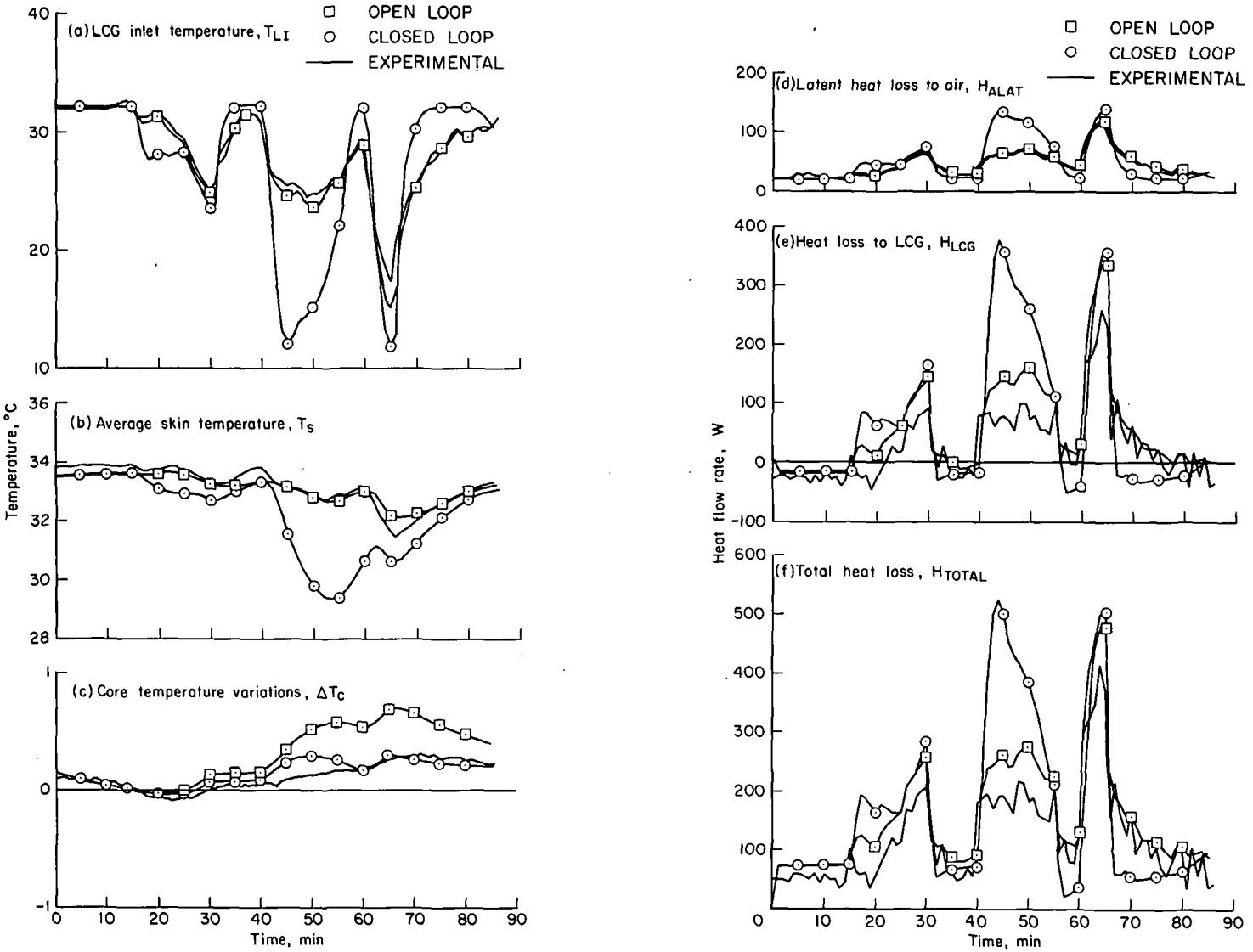

Figure 31.– CSMP simulations; activity schedule VI (treadmill speeds: 1/2 – 1-1/2, 1-1/2 – 1/2, 2 m/sec).

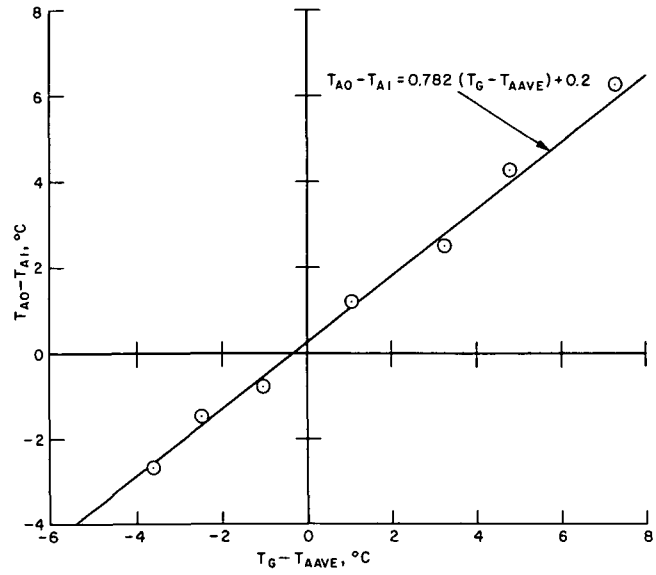

Figure 32.– Temperature rise through AVG – manikin test.

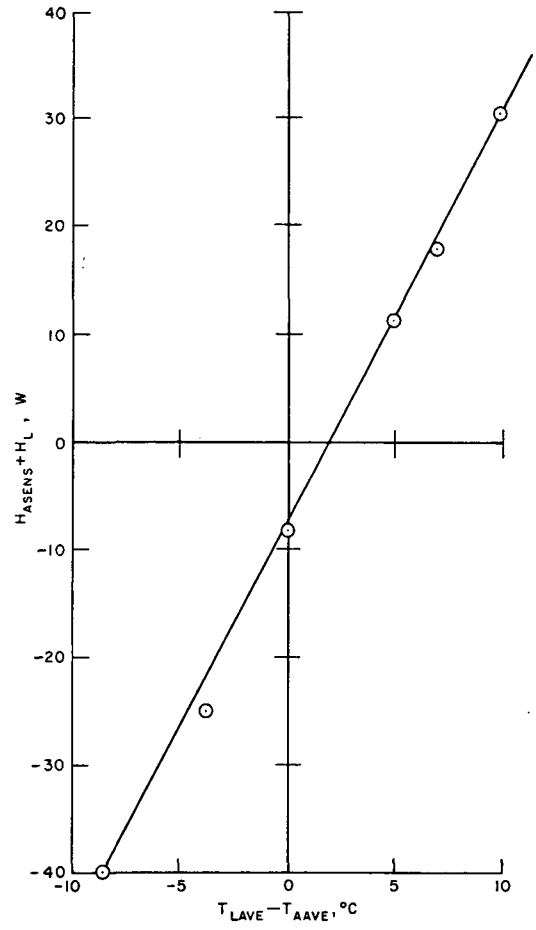

Figure 33.– Heat transfer rate to ventilating air – wrapped manikin test.

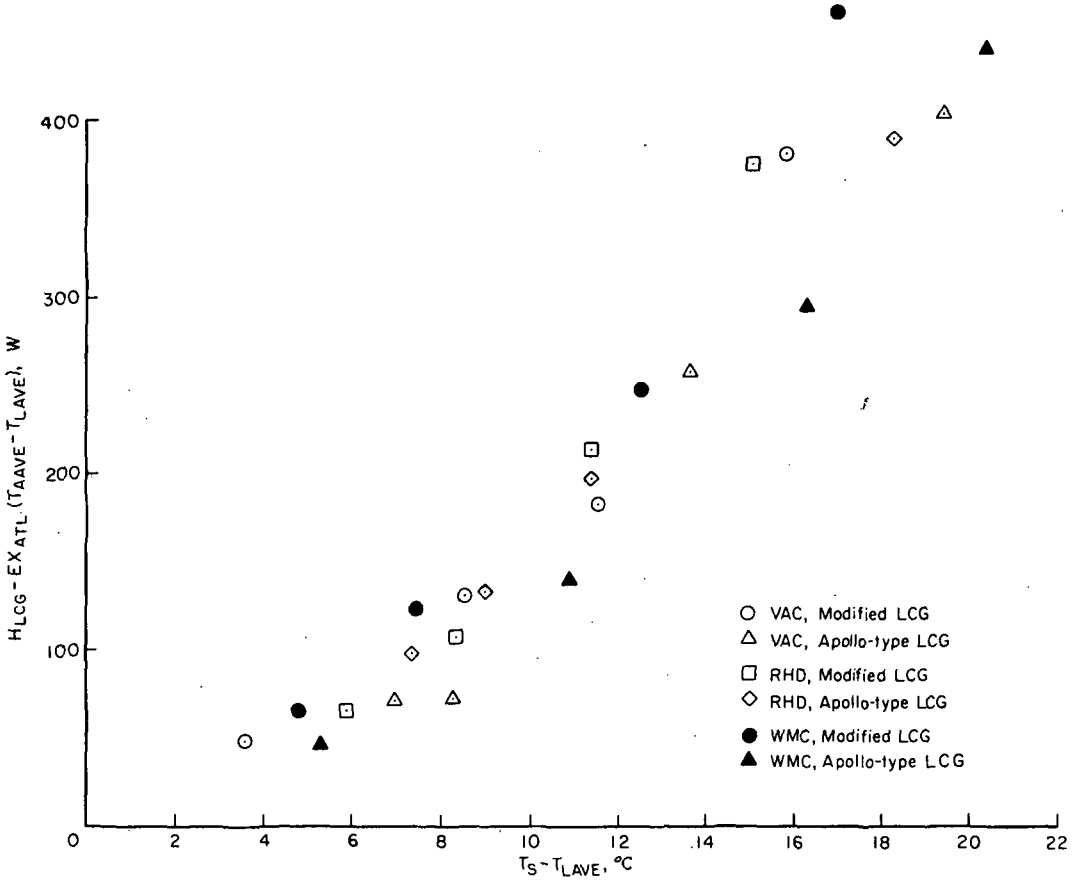

Figure 34.– Heat transfer rate between skin and LCG.

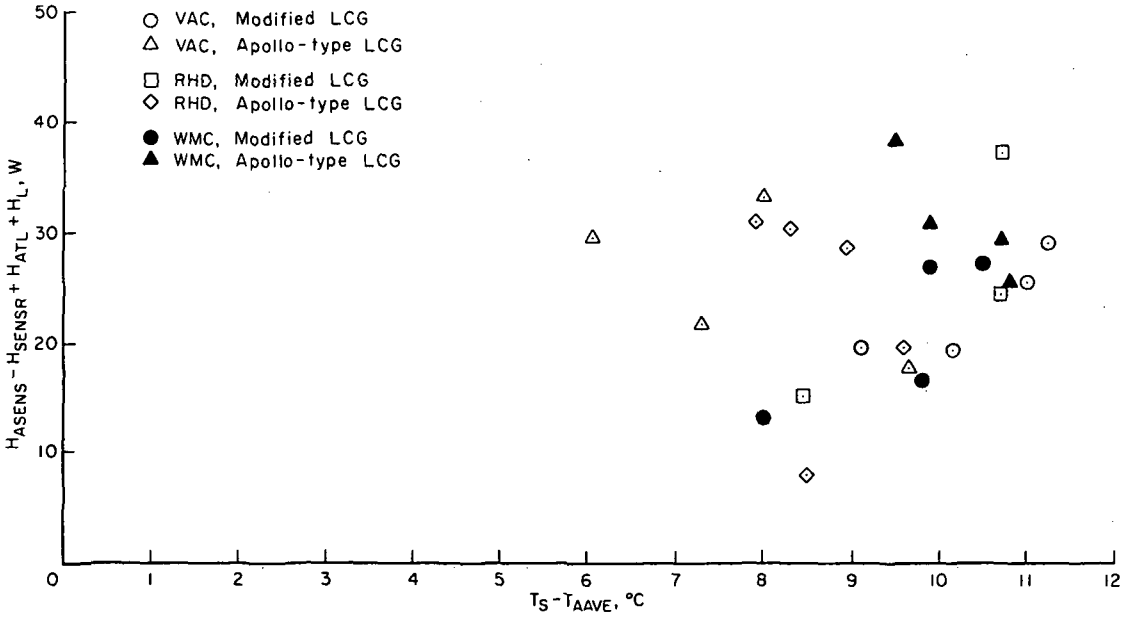

Figure 35.– Heat transfer rate between skin and ventilating air.

"The aeronautical and space activities of the United States shall be conducted so as to contribute . . . to the expansion of human knowledge of phenomena in the atmosphere and space. The Administration shall provide for the widest practicable and appropriate dissemination of information concerning its activities and the results thereof."

—NATIONAL AERONAUTICS AND SPACE ACT OF 1958

NASA SCIENTIFIC AND TECHNICAL PUBLICATIONS

TECHNICAL REPORTS: Scientific and technical information considered important, complete, and a lasting contribution to existing knowledge.

TECHNICAL NOTES: Information less broad in scope but nevertheless of importance as a contribution to existing knowledge.

TECHNICAL MEMORANDUMS: Information receiving limited distribution because of preliminary data, security classification, or other reasons. Also includes conference proceedings with either limited or unlimited distribution.

CONTRACTOR REPORTS: Scientific and technical information generated under a NASA contract or grant and considered an important contribution to existing knowledge.

TECHNICAL TRANSLATIONS: Information published in a foreign language considered to merit NASA distribution in English.

SPECIAL PUBLICATIONS: Information derived from or of value to NASA activities. Publications include final reports of major projects, monographs, data compilations, handbooks, sourcebooks, and special bibliographies.

TECHNOLOGY UTILIZATION PUBLICATIONS: Information on technology used by NASA that may be of particular interest in commercial and other non-aerospace applications. Publications include Tech Briefs, Technology Utilization Reports and Technology Surveys.

Details on the availability of these publications may be obtained from:

SCIENTIFIC AND TECHNICAL INFORMATION OFFICE

NATIONAL AERONAUTICS AND SPACE ADMINISTRATION

Washington, D.C. 20546